

1 **Interacting effects of fire and hydroclimate on oak and beech**
2 **community prevalence in the southern Great Lakes region**

3 **Abstract**

4 1. Rising temperatures, increasing hydroclimate variability, and intensifying disturbance regimes
5 increase the risk of rapid ecosystem conversions. We can leverage multi-proxy records of past
6 ecosystem transformations to understand their causes and ecosystem vulnerability to rapid
7 change.

8 2. Prior to Euro-American settlement, northern Indiana was a mosaic of prairie, oak-dominated
9 forests/woodlands, and beech-dominated hardwood forests. This heterogeneity, combined with
10 well-documented but poorly understood past beech population declines, make this region ideal
11 for studying the drivers of ecosystem transformations.

12 3. Here we present a new record from Story Lake, IN, with proxies for vegetation composition
13 (pollen), fire (charcoal), and beech intrinsic water use efficiency ($\delta^{13}\text{C}$ of beech pollen; $\delta^{13}\text{C}_{\text{beech}}$).
14 Multiple proxies from the same core enable clear establishment of lead-lag relationships.
15 Additionally, $\delta^{13}\text{C}_{\text{beech}}$ enables direct comparisons between beech population abundance and
16 physiological responses to changing environments. We compare Story Lake to a nearby lake-level
17 reconstruction and to pollen records from nearby Pretty and Appleman Lakes and the distal Spicer
18 Lake, to test hypotheses about synchrony and the spatial scale of governing processes.

19 4. The 11.7 ka sediment record from Story Lake indicates multiple conversions between beech-
20 hardwood forest and oak forest/woodland. Beech pollen abundances rapidly increased between
21 7.5 and 7.1 ka, while oak declined. Oak abundances increased after 4.6 ka and remained high until
22 2.8 ka, indicating replacement of mesic forests by oak forest/woodland. At 2.8 ka, beech
23 abundances rapidly increased, indicating mesic forest reestablishment. Beech and oak

24 abundances correlate with charcoal accumulation rates but beech abundance is not correlated
25 with $\delta^{13}\text{C}_{\text{beech}}$.

26 5. Fluctuations in beech abundances are synchronous among Story, Appleman, and Pretty Lakes, but
27 asynchronous between Story and Spicer Lakes, suggesting regulation by local-scale vegetation-
28 fire-climate feedbacks and secondarily by regional-scale drivers.

29 6. Holocene forest composition and fire dynamics appear to be closely co-regulated and may be
30 affected by local to regional climate variations. The importance of extrinsic drivers and
31 positive/negative feedbacks changes over time, with higher ecoclimate sensitivity before 2.8 ka
32 and greater resilience afterwards.

33 7. *Synthesis*: Overall, oak- and beech-dominated ecosystems were highly dynamic over the
34 Holocene, with multiple ecosystem conversions driven by shifting interactions among vegetation,
35 hydroclimate, and fire regime.

36 **Key Words**

37 Aridity, *Fagus grandifolia*, *Quercus*, Holocene, disturbance regime, fire, hydroclimate, drought, pollen,
38 stable carbon isotopes, lake-level, palaeoecology, rapid ecological change

39 **Introduction**

40 Much of the current literature on forest transformations driven by rising temperatures, increasing
41 hydroclimate variability, and changes disturbance regimes has focused on areas that experience frequent
42 drought or fires, such as the western US (Westerling et al. 2011, Romme et al. 2011, Hartmann et al. 2018,
43 Allen et. al 2015), or in high-latitude regions where species and ecosystem distributions are closely
44 regulated by temperature (Payette 2021). Palaeoecological evidence can provide a deeper time
45 perspective of these dynamics by helping further our understanding of rapid population fluctuations and
46 corresponding ecosystem transitions, including in areas that are today seemingly resilient. In the Great
47 Lakes region, mesic tree taxa have experienced multiple abrupt population declines during the Holocene
48 and provide a rich study system for understanding past rapid vegetation changes (Shuman et al. 2009,
49 Shuman 2012, Booth et al. 2012a, Booth et al. 2012b, Wang et al. 2016). For example, the range-wide
50 population collapse of eastern hemlock (*Tsuga canadensis*) at 5.5 to 5.3 thousand years before present
51 (ka BP) has been extensively studied and is often associated with one or more severe drought events
52 suggesting high sensitivity to hydroclimatic variation (Shuman et al. 2009, Shuman 2012, Oswald and
53 Foster 2012, Booth et al. 2012a). However, other causes of the eastern hemlock collapse have been
54 suggested including regional temperature changes (Shuman et al. 2023) and outbreaks of hemlock looper
55 or other pests or pathogens (Bhiry and Filion 1996).

56 American beech (*Fagus grandifolia*, herein beech), another common mesic tree species in the eastern US,
57 has undergone rapid population fluctuations throughout the Holocene (Booth et al. 2012b, Wang et al.
58 2016), but the patterns and causes are less well studied. After the last glacial maximum, beech expanded
59 northward from the southeastern US, reaching the Great Lakes region between 8.0 and 6.0 ka (Williams
60 1974, Bernabo and Webb 1977, Davis 1981, Webb et al. 1984, Bennett 1985, Bennett 1988). After
61 establishment in the Great Lakes region, beech populations experienced repeated declines across sites in

62 Ohio, Indiana (IN), Michigan (MI), and Wisconsin (Wang et al. 2016). At Spicer Lake, IN, beech populations
63 rapidly expanded at 6.8 ka and subsequently ranged from near 30% to <5% pollen abundance (Wang et
64 al. 2016). Beech populations at Spicer Lake experienced five abrupt and well-dated declines (5.3 ka, 4.3-
65 4.0 ka, 3.2–2.0 ka, 1.2 ka, 1 ka), all followed by abrupt increases, except for the decline at 1 ka, from which
66 beech has not recovered (Wang et al. 2016).

67 Better constraints on the timing of the beech declines across sites is essential to testing causal hypotheses.
68 The declines at Spicer Lake appear to be asynchronous with declines at other sites in the Great Lakes
69 region (Wang et al. 2016). However, this apparent asynchrony could be caused by poor dating constraints,
70 as many records were collected decades ago and rely on relatively few bulk-sediment radiocarbon dates,
71 which are prone to biasing due to hardwater effects (Grimm et al. 2009). Synchronous beech declines
72 across the region would suggest macro-scale extrinsic drivers, such as temperature variations or pest
73 outbreaks, as has been invoked for eastern hemlock (Shuman et al. 2009, Booth et al. 2012a, Shuman et
74 al. 2023). Asynchronous beech variations would suggest localized interactions between extrinsic, intrinsic,
75 and disturbance processes, such as localized shifts in fire regime, local hydroclimate variability, or species
76 interactions leading to shifts in the dominant taxon. Cross-scale interactions are also possible, e.g. local-
77 scale feedbacks interacting with macro-scale extrinsic drivers, creating sub-regional temporal mosaics
78 with clusters of synchronized declines (Williams et al. 2011). These intrinsic and extrinsic processes can
79 further interact with disturbance regimes to amplify or mitigate rates of ecological change (Ratajczak et
80 al. 2018) with transition zones between ecosystems being particularly susceptible to rapid changes in
81 community composition (Nelson and Hu 2008, Williams et al. 2009, Hupy and Yansa 2009, Wiles 2023).

82 The thin bark of beech makes it vulnerable to damage by fire, while a shallow root system also makes it
83 susceptible to changes in soil moisture (Tubbs and Houston 1990). During the Medieval Climate Anomaly
84 (1.05 to 0.6 ka BP), beech declines were associated with increased fire frequency at some sites in northern
85 Michigan (Booth et al. 2012b), but at Spicer Lake there was largely no consistent relationship between

86 beech abundance and fire (Wang et al. 2016). At some sites, fire regimes can stabilize vegetation
87 composition. For example, in Minnesota's Big Woods the late-Holocene shift from oak woodland to mesic
88 forest only occurred at the sites where fire was absent due to the presence of natural firebreaks (Calder
89 2016, Grimm 1984). Drought could also cause beech declines, but the Spicer Lake record lacks robust
90 paleohydrology proxies (Wang et al., 2016). More independent paleohydrology proxies are needed, such
91 as past lake level variations (Digerfeldt et al. 1993, Pribyl and Shuman 2014) or other indicators of the
92 regional moisture balance to further evaluate the relationship between beech declines and hydroclimatic
93 history (Booth 2008, Adams et al. 2015). Variations in beech abundances may also be affected by changes
94 in temperature, which appear to have affected the region during the Holocene (Puleo et al., 2020; Shuman
95 et al., 2023), and pathogen outbreaks, which are known from modern forests. For example, some studies
96 attribute late-Holocene declines in beech in New England and the Great Lakes region to Little Ice Age
97 cooling (Fuller et al., 1998; Gajewski, 1987), whereas the accidental introduction of beech bark disease to
98 the US in the 1890s CE has devastated many beech forests, with mortality rates of 50% and infestation
99 rates of 80 to 95% (Stephanson and Coe, 2017; Beckman et al. 2021).

100 Even with independent proxies of hydroclimate variation, the potential for different sensitivities and
101 response times between lacustrine and terrestrial ecosystems remains a source of uncertainty. A
102 relatively new approach that integrates the balance between carbon and water fluxes and thus shows
103 promise for inferring shifts in the physiological sensitivity and response time of vegetation to climate
104 forcing is stable carbon isotopic ($\delta^{13}\text{C}$) analyses of fossil pollen grains of C_3 plants (Jahren 2004; Loader
105 and Hemming 2004; Griener et al. 2013, Nelson 2012). The $\delta^{13}\text{C}$ values provide a seasonally-integrated
106 signal of intrinsic water use efficiency (iWUE), which is the ratio of photosynthesis and stomatal
107 conductance of water (Farquhar et al., 1989). In terms of water-use strategies, plants that prioritize carbon
108 gain relative to water loss have low iWUE and $\delta^{13}\text{C}$ values, whereas those that prioritize water
109 conservation relative to carbon gain have high iWUE and $\delta^{13}\text{C}$ values (Bacon, 2009; Farquhar and Sharkey,

110 1982), and dry conditions tend to favor the latter (Sperry et al., 2017). Atmospheric CO₂, atmospheric
111 pollution, and climate (temperature and precipitation) have been shown to affect plant iWUE during the
112 historical record via their influences on photosynthesis and/or stomatal conductance (Mathias et al.,
113 2023), though the former two factors are unlikely to have been significant controls of iWUE during the
114 Holocene prior to the industrial revolution. Pollen $\delta^{13}\text{C}$ values ($\delta^{13}\text{C}_{\text{pollen}}$) represent landscape- to
115 population-level shifts in iWUE because multiple pollen grains must be combined to produce enough
116 carbon for $\delta^{13}\text{C}$ analysis and each sediment sample comprises pollen grains from many individual plants
117 within pollen source radii on the order of 10s of km (Prentice 1988). The $\delta^{13}\text{C}$ data from specific taxa can
118 be coupled with pollen assemblage data to assess the influence of variations in iWUE on abundance
119 changes for individual taxa and changes in community composition (Griener et al. 2013).

120 Here we seek to better understand the drivers of rapid changes in beech abundances in the southern
121 Great Lakes region, through a new well-dated, multi-proxy record for Story Lake, Indiana. This record
122 includes proxies for past vegetation composition (pollen), iWUE of beech ($\delta^{13}\text{C}_{\text{beech}}$), and fire regime
123 (charcoal) from the same core. The Story records are compared to a recent lake level reconstruction from
124 nearby Lake Lavine, MI (Ray-Cozzens 2023) as an independent indicator of past hydroclimate variations.
125 We also compare the history of beech variations at Story with those at two nearby sites within 15 km of
126 Story Lake (Appelman and Pretty Lakes), and one more distal lake located 120 km to the west (Spicer
127 Lake). These comparisons allow us to test hypotheses about the synchrony of vegetation changes at
128 landscape to regional scales and thereby assess the relative importance of local-scale vegetation-fire-
129 climate feedbacks and regional-scale climatic drivers on rapid changes in mesic tree populations in the
130 southern Great Lakes region.

131 **Materials and Methods**

132 **Site Description**

133 Our main study site, Story Lake (41.51237, -85.13500) is located in DeKalb County, northern Indiana (Fig. 1). Comparison pollen sites are also located in northern Indiana, including a new Holocene pollen record for previously studied Appleman Lake (Gill et al. 2009) and preexisting records from the Neotoma Paleoecology Database for Pretty Lake (Williams 1974) and Spicer Lake (Wang et al., 2016) and a comparison hydrological reconstruction located in southern Michigan from Lake Lavine (Ray-Cozzens 2023; Fig. 1). This region is situated in complex mosaic of three ecosystems: the prairie peninsula in the southwest, oak-dominated forest and woodlands in portions of the north, east, and west and beech-dominated forests in portions of the north, south and east (Fig. 1, McNab et al. 2007, Paciorek et al. 2016, Landfire 2020, Transeau 1935). Therefore, this area contains two major ecosystem transitions: the prairie-forest transition (Fig. 1a), whose Holocene dynamics that have been widely studied (e.g. Nelson and Hu 2008, Williams et al. 2009) and the oak-beech transition which is much less well studied (Fig. 1b, 1c, Abrams and Nowacki 2019, Wang et al. 2016). This makes northern Indiana an ideal region for studying the importance of the drivers of rapid vegetation shifts in complex ecosystem mosaics in the Great Lakes region and how they vary in time and space.

147 Pre-settlement vegetation of northern Indiana was a mosaic of oak-hickory and beech-maple forests with 148 patches of wetland and prairie communities (Lindsey et al. 1965). Beech was a prominent taxon in these 149 pre-settlement forests in northeastern Indiana as well as mid to late Holocene forests of southern Ontario, 150 but it experienced widespread losses with Euro-American land conversion (Fig. 1; Paciorek et al. 2016, Lindsey et al. 1965, Bennett 1987). Contemporary mixed forests in northern Indiana are generally 152 characterized by a mosaic of the maple-beech-birch, oak-hickory, and elm-ash-cottonwood communities 153 (McNab et al. 2007). Elsewhere in the Great Lakes and northeastern North America, beech-dominated

154 mixed forests are compositionally diverse and associated with both fine-grained soils that retain moisture
155 and low frequency fire disturbance (Abrams and Downs 2011, Engstrom et al. 1984, Henne et al., 2007,
156 Landfire 2020, Lindsey et al. 1965). Oak communities in northeastern Indiana and elsewhere range from
157 closed forests to open woodlands or prairies and are mostly found in xeric sites, often having well drained
158 sandy soils, and are adapted to frequent low intensity fire regimes (Landfire 2020, Lindsey et al. 1965,
159 Bennett 1987). However, both oak and beech forests prevail on the silt loams that are the dominant soils
160 type in northern Indiana (Lindsey et al. 1965). The gradient between closed forests and open woodland in
161 northern Indiana is also largely controlled by fire frequency and intensity, with frequent fire promoting
162 oak woodlands while locations with low fire-return intervals allow for fire-sensitive species to dominate
163 the overstory (Henderson and Long 1984). More broadly, semi-arid ecosystems in the Great Lakes region
164 have been governed throughout the Holocene by feedbacks between aridity, vegetation composition, and
165 fire regime, driving community shifts from fire-tolerant oak woodland and prairie systems to fire-
166 intolerant mesic forests (Grimm 1983, Nelson et al. 2006, Nelson and Hu 2008, Shuman et al. 2009).

167 The climate of the southern Great Lakes region is continental with warm summers and cold winters, with
168 northeastern Indiana experiencing monthly average temperature ranging from -4.6°C to 21.7°C with 988
169 mm annual precipitation (NOAA 2023). This region also has a large range of annual snowfall with some
170 areas receiving high levels of lake effect snow, up to 70%, with annual snowfall between 60 and 80 inches
171 on eastern shore of Lake Michigan with less snowfall inland. Annual snowfall near Story Lake averages 40
172 inches (NOAA 2023) and typically 30-50% of annual snowfall comes from lake effect snow (Jones et al.
173 2022).

174 Story Lake is a 30-ha kettle lake (Fig. 1), likely formed by remnant glacial ice embedded into glacial till
175 from the Huron-Erie lobe during the retreat of the Laurentide Ice Sheet (Gray 1989). The terrain
176 surrounding Story Lake is flat with small hills. Story Lake has two small islands and is connected by a
177 narrow marsh and stream to an adjacent Lower Story Lake. Story Lake has no inlet stream. Soil conditions

178 range from fine-loam near the basin to fine to coarse-loam in the uplands (Soil Survey 2023). Forests
179 border the lake to the north and west with a mosaic of agricultural fields in the surrounding area.
180 Additionally, residential houses and a camping resort border the southeastern portion of the lake (Fig. 1).
181 Coring took place in June 2019 with the coring site located in the southern part of the lake, near the
182 deepest part of the lake based on field depth surveys and pre-existing bathymetry maps (Fig. 1). The water
183 depth at the coring location was 8.8 meters. We retrieved three closely adjacent and drive-offset cores,
184 each 1-meter in length, extending from the sediment-water interface to basal glacial till. The top drive
185 used a modified Livingston with a polycarbonate Bolivian adaptor and the remaining drives were extracted
186 using the modified-Livingston steel barrel, with mud extruded after coring into PVC pipe for transport.
187 Cores were taken to the Continental Scientific Drilling Facility at the University of Minnesota-Twin Cities
188 for longitudinal splitting, high-resolution photographing, and logging for bulk density and magnetic
189 susceptibility. After splitting and imaging, a 11.2 meter composite core was created by matching
190 stratigraphy across cores to avoid samples at core breaks where possible. At the University of Wisconsin-
191 Madison, the composite core was divided into 1 cm segments, from which all subsequent samples were
192 obtained.

193 **Radiocarbon dates and age-depth model**

194 To create the Story Lake age-depth model, we submitted 16 terrestrial plant macrofossils for radiocarbon
195 dating to the W. M. Keck Carbon Cycle Accelerator Mass Spectrometry Laboratory (Keck-CCAMS) at the
196 University of California, Irvine (Table 1). One sample was determined to be too small for AMS analysis
197 (642.5 cm, Table 1). The age-depth model was generated in R (R Core Team 2021) using the package
198 *bchron* version 4.7.6 (Haslett and Parnell 2008). Of the 15 radiocarbon samples, two samples from near
199 the top of the core were determined to be modern, and so likely contained excess ^{14}C from thermonuclear
200 weapons testing (Table 1). To determine the age of those samples, the program *CALIBomb* was used

201 (Reimer and Reimer 2023) and ages are reported in calibrated years as the mean of the 98% confidence
202 interval and error estimates from the 95% confidence curve. For both modern samples, this equated to
203 an age of 1971 CE \pm 12 years (Reimer and Reimer 2023). In addition to the radiocarbon dates, we used
204 two age controls: the core top (set to 2019 CE \pm 10 years, to represent uncertainty in sediment mixing)
205 and the sharp increase of ragweed (*Ambrosia*) pollen relative abundances at 128.5 cm as an indicator of
206 Euro-American land clearance. Indiana was actively settled between 1810 and 1870, with the largest rates
207 of forest cutting between 1870 and 1910 CE, after the advent of the sawmill in 1860 CE (Denuy 1953).
208 We thus set the ragweed peak to 1860 CE \pm 25 years to capture the full range of intense land clearing in
209 Indiana. Age uncertainties for the two modern samples, core top, and ragweed rise were represented by
210 a normal distribution and the uncertainties for the remaining 13 radiocarbon samples were estimated
211 using the IntCal20 calibration curve (Reimer et al. 2020).

212 **Laboratory Analyses: Pollen, Charcoal, and Carbon Isotopes**

213 Pollen and charcoal analysis for Story Lake were performed at the University of Wisconsin-Madison.
214 Sediment samples for pollen analysis were sampled using a 1 cm³ metal sampler at 8-cm intervals and up
215 to 4-cm intervals (average time interval: 85 \pm 38 years). Pollen samples were processed to remove
216 carbonates (10% hydrochloric acid), silicates (48% hydrofluoric acid), and organic matter (10% potassium
217 hydroxide) and acetalize the pollen grains for identification following standard methods (Faegri and
218 Iversen 1984). Processed pollen samples were analyzed at 400x magnification using a Zeiss Axiolab 5
219 microscope, pollen grains were identified using the reference key and images in Kapp et al. (2000), and at
220 least 300 terrestrial pollen grains were identified for each sample. Pollen percentages were calculated
221 using the sum of terrestrial pollen grains in R (R Core Team 2021) and graphical representation was
222 completed the R package *riojaPlot* (Juggins 2022).

223 Macroscopic charcoal in sediment cores is used as a proxy for fire history (Whitlock and Larson 2001,
224 Higuera et al. 2009, Higuera et al. 2010). Macroscopic charcoal was sampled contiguously with 1 cm³
225 subsamples from core top to 746 cm, to encompass the times when beech was abundant near Story Lake.
226 Sediment was treated with 6% hydrogen peroxide solution to oxidize organic matter and sodium
227 hexametaphosphate to disaggregate clay particles, then heated at 50°C for 24-hours. Samples were then
228 sieved using a 125-micron mesh, material remaining on the sieve was rinsed into petri dishes, liquid was
229 evaporated in a drying oven for 12-48 hours, and all pieces of charcoal were counted using 40x
230 magnification. To calculate charcoal accumulation rates (pieces cm⁻² year⁻¹), charcoal concentrations
231 (pieces cm⁻³) were multiplied by the sediment accumulation rate obtained from the age-depth model (cm
232 year⁻¹) for each depth. The signal-to-noise ratio was calculated using the R package *tapas* (Finsinger and
233 Bonnici 2022)

234 The $\delta^{13}\text{C}$ analysis of beech pollen was performed at the University of Maryland Center for Environmental
235 Science. Because of the effort involved, this analysis was only performed for samples younger than 5.0 ka
236 BP. Sediment samples were processed to extract pollen grains using methods designed to avoid using
237 carbon-containing chemicals (Nelson et al. 2006). To enable accurate and precise $\delta^{13}\text{C}$ analysis (Korasidis
238 et al. 2022), aliquots of 15-20 beech pollen grains were extracted from each sample using an Eppendorf
239 Transferman micromanipulator and rinsed in nanopure water at 200x magnification on a microscope slide.
240 These grains were applied in a ~0.5 μl drop of nano-pure water to a spooling-wire micro-combustion
241 device interfaced with an isotope-ratio mass spectrometer (SWiM-IRMS; Nelson 2012). Blanks (nano-pure
242 water to which pollen grains were added and subsequently removed) were analyzed along with aliquots;
243 in all cases the CO₂ yield of the pollen-containing aliquots was > 5x those of the blanks. Sample data were
244 normalized to Vienna Peedee Belemnite using $\delta^{13}\text{C}$ measurements of 5 nmol C of dissolved in-house
245 standards (leucine and sorbitol) that were previously calibrated to USGS40 and USGS41. Between one and
246 six aliquots of beech pollen were analyzed from each sample depth and their $\delta^{13}\text{C}$ values were averaged.

247 These individual aliquot measurements provide a measure of uncertainty that combines both analytical
248 uncertainty (which is $\pm 1\%$ or lower; Korasidis et al. 2022) and random variations in the $\delta^{13}\text{C}$ of the
249 population of beech pollen grains drawn for isotopic analysis. Overall, we analyzed 101 aliquots across 44
250 samples.

251 **Numerical Analyses**

252 To determine changes in the prevalence of vegetation types through time, we used topic analysis, a
253 machine-learning approach that categorizes taxa into assemblages and provides an estimate of the
254 prevalence of each assemblage (Blei 2012). Topic analysis was originally developed for text mining, where
255 documents are analyzed for patterns of associations among terms, based on iterative random draws
256 from a statistical distribution (we used logistic normal distribution, see below). Associated terms within
257 those documents are placed in groups, called topics, and then the prevalence of topics within documents
258 becomes a primary way of describing documents. Topic analysis carries advantages for ecological
259 applications due to its ability to provide robust and interpretable results, even for data with uneven
260 sampling or for datasets with many variables or non-linear relationships among variables (Blei 2012, Valle
261 et al. 2014, Christensen et al. 2018).

262 Topic analyses applied to ecological community data have two components: an estimate of importance
263 of each taxon within an ecological community (beta) and an indication of the prevalence of each ecological
264 community at a spatiotemporal locus (gamma). Topic analysis is thus very similar conceptually to standard
265 ordination methods in ecology. For fossil pollen records, time series of gamma can provide information
266 about shifts in prevalence of vegetation types.

267 Within topic analysis, two main algorithms can be used to categorize taxa into ecological communities:
268 latent Dirichlet allocation (LDA) and correlated topic model (CTM). These two methods mainly differ with
269 respect to the statistical distribution used to model variability among topics: LDA uses a Dirichlet

270 distribution while CTM uses a logistic normal distribution (Blei et al. 2003, Blei and Lafferty 2006). The
271 Dirichlet distribution in LDA assumes that all topics are strongly independent, which is typically violated
272 by ecological communities, given species interactions and shared responses to common environmental
273 drivers. In contrast, the logistic normal distribution in CTM contains a correlation matrix that accounts for
274 correlation among ecological communities. Therefore, the CTM method was used here. In CTM the user
275 must specify how many topics to use; here we explored CTM with three to eight vegetation types and
276 present the results for three vegetation types in the main text and alternate versions in Supplementary
277 Information. All analysis was performed in R using the package *topicmodels* (Grün and Hornik 2011, Grün
278 and Hornik 2023) using suggested control values from Grün and Hornik (2011).

279 Bayesian Change Point detection (BCP) for the gamma time series produced by the CTM analysis was used
280 to determine the timing of rapid community shifts. BCP identified changes in prevalence of ecological
281 communities, as identified as posterior probabilities of greater than 0.5, were interpreted as periods of
282 rapid ecological community shifts. BCP analysis was performed using the R package *bcp* (Erdman and
283 Emerson 2007).

284 **Comparison Site Records**

285 Appleman Lake, IN (41.6237, -85.2136) is a 21-ha kettle pond located 14 km northwest of Story Lake (Fig
286 1). Appleman Lake was cored in 2005 and the deglacial portion of the core was processed and analyzed
287 by Gill et al. (2009). For this paper, we present a new pollen record for the Holocene portion of the core.
288 The portion of the from 673 cm to the core top was subsampled at 8 cm resolution and processed for
289 pollen analysis using the same technique as for Story Lake. Pollen was identified and counted at the
290 University of Minnesota. The Holocene age-depth model for Appleman was based on the youngest two
291 radiocarbon dates from Gill et al. (2009) at 627.5 cm (8397 calibrated years BP) and 618.5 cm (8106
292 calibrated years BD), the ragweed rise at 40.5 cm (1860 CE consistent with Story Lake), and core top (2005

293 CE). The age-depth model was generated using *bchron* version 4.7.6 (Haslett and Parnell 2008). Pretty
294 Lake, IN (41.5760, -85.2498) is a 74.5 ha lake located 12 km northwest of Story Lake (Fig 1; Williams 1974).
295 Spicer Lake, IN (41.7478, -86.5219) is a 5-ha kettle lake located 120 km west of Story Lake (Fig 1; Wang et
296 al. 2016). Pollen and radiocarbon data for Pretty and Spicer Lakes were downloaded from the Neotoma
297 Paleoecology Database (Williams et al. 2018) and their age-depth models were rebuilt using *bchron*
298 version 4.7.6 (Haslett and Parnell 2008). Lake Lavine, MI (41.7693, -85.0376) is an 87-ha lake located 30
299 km north of Story Lake and was used as a hydrological comparison to Story Lake (Fig. 1). The lake level
300 reconstruction for Lake Lavine was conducted by Ray -Cozzens (2022).

301 **Results**

302 **Age depth model**

303 The final age-depth model spans from 11.7 ± 0.6 ka BP (thousands of years before radiocarbon present,
304 i.e. 1950 CE) to 2019 CE, however, we were unable to retrieve a basal date due to lack of dateable material
305 in the last 300 cm of the composite core (Fig. 2). Sedimentation rates are nearly constant through much
306 of the record, with an average sedimentation rate of $0.11 \text{ cm year}^{-1}$ (deposition time of $8.93 \text{ years cm}^{-1}$).
307 However, near the top of the core, at 0.2 ka BP (138.5 cm), the sedimentation rate increases to an average
308 of $0.63 \text{ cm year}^{-1}$ (deposition time decreases to $1.6 \text{ years cm}^{-1}$) (Fig. 2). See Supplementary Information
309 for the *bchron* age-depth models for Spicer, Pretty, and Appleman Lakes.

310 **Vegetation History**

311 Pre-settlement vegetation changes at Story Lake were dominated by three taxa, beech (*Fagus*), oak
312 (*Quercus*), and elm (*Ulmus*). Beech pollen abundances began to increase at 7.5 ka BP, with an acceleration
313 at 7.1 ka BP, increasing from 5% to 25% over approximately 300 years (Fig. 3). During this initial increase,
314 abundances of oak pollen declined from 57% at 7.9 ka BP to a low of 25% at 6.6 ka BP (Fig. 3). From 6.6
315 ka BP to 4.6 ka BP, oak abundances generally increased while beech decreased, with large centennial scale

316 variations superimposed on these millennial scale trends. From 4.6 ka BP to 3.0 ka BP, beech remained
317 low while oak reached its highest abundance of 61% at 4.3 ka BP. At 3.0 ka BP, beech abundances started
318 to rapidly increase from 3% to 22% in approximately 400 years, while oak decreased (Fig. 3). Starting at
319 2.6 ka BP, both beech and oak abundances fluctuated (e.g. beech varied from a high of 27% to a low of
320 7%) around a relatively constant mean, until the Euro-American intensification of land use at 0.09 ka BP
321 where both taxa abundances declined and have not recovered.

322 During the middle Holocene (8.0 to 5.0 ka), elm composed a substantial part of the pollen assemblage,
323 ranging from 12% to 28% with a mean of 18% (Fig. 3). After 5.0 ka BP, elm abundances declined but
324 fluctuated from 2% to 12% with a mean of 7% (Fig. 3). This pattern is consistent with other regional
325 records, where elm reached maximum abundance during the early to middle Holocene, perhaps due to
326 increased summer insolation (Wang et al. 2016, Williams and Jackson 2007). Other notable hardwood
327 taxa at Story Lake include hickory (*Carya*), hornbeam (*Ostrya/Carpinus*), ash (*Fraxinus*), walnut (*Juglans*),
328 sycamore (*Platanus*), and maple (*Acer*) (Fig. 3). These taxon abundances fluctuated but typically each were
329 <10% of the pollen assemblage (Fig. 3). Sycamore was generally more abundant in the middle Holocene
330 and decreases in the late Holocene. Hickory, ash, and maple conversely, were low during the middle
331 Holocene, then became more abundant in the late Holocene (Fig. 3). Both hornbeam and walnut remained
332 consistently low throughout the entire record (Fig. 3).

333 Herbaceous taxa were uncommon at Story Lake, except for ragweed (*Ambrosia*), which reached >40%
334 abundance in response to Euro-American land clearance (Fig. 3). Grass (Poaceae) first modestly increased
335 at 5.2 ka, then was moderately abundant after 3.0 ka BP, comprising approximately 5% of the pollen
336 assemblage until Euro-American land clearance, after which grass increased to its maximum abundance
337 of 15% at 0.0 ka BP (1950 CE, Fig. 3). Total non-arboreal pollen also peaked in response to Euro-American
338 land clearance with non-arboreal pollen dominating the assemblage at 0.01 ka BP (arboreal:non-arboreal
339 ratio = 0.67).

340 Three vegetation types, as determined by topic analysis, were robust to the choice of total number of
341 vegetation types: beech-hardwood forest, oak forest/woodland, and open and cleared vegetation (Fig. 4,
342 Supplementary Information). Vegetation types identified beyond these three generally further
343 differentiate the oak forest/woodland into various communities that have oak as the dominant taxa but
344 with different secondary taxa, while continuing to identify the beech-hardwood forest and open and
345 cleared communities (Supplementary Information). One exception is the five topic model, which
346 combines beech, oak, and elm into one community (Supplementary Information). However, the five-topic
347 results have the worst model fit (highest AIC and BIC, Supplementary Information). The results for three
348 vegetation types were chosen for further discussion here, with other variants available in Supplemental
349 Information.

350 *Beech-hardwood forest*: This vegetation type is dominated by beech (β = 0.34), with elm and oak as
351 secondary taxa (β = 0.20 and 0.12 respectively, Fig. 4b). Other important taxa include ash (β = 0.08)
352 and sycamore (β = 0.07, Fig. 4b). This vegetation type is similar to the elm-ash-cottonwood vegetation
353 type currently found in northern Indiana (McNab et al. 2007) as well as with pollen records from other
354 beech forests in southern Ontario (Bennett 1987). Although cottonwood (*Populus*) pollen is not prevalent
355 in the Story Lake pollen record, this modern vegetation type also contains sycamore and beech, which is
356 consistent with the Holocene pollen record at Story Lake (Fig. 3). Over the Holocene, the prevalence of
357 beech-hardwood forest changed rapidly five times, with two increases in prevalence (7.1 ka BP, and 2.8
358 ka BP) and three decreases (6.1 ka BP, 4.6 ka BP, and 0.02 ka BP).

359 *Oak forest/woodland*: This vegetation type is strongly associated with oak (β = 0.57), with hickory and
360 elm as secondary taxa (β = 0.08 and β = 0.07 respectively) (Fig. 4c). This vegetation type is similar
361 to the oak-hickory vegetation type currently associated with northern Indiana, which is defined as having
362 >50% of vegetation cover as oak and hickory (McNab et al. 2007). At Story Lake, the prevalence of oak
363 forest/woodland changed rapidly five times, with timings that are synchronous with and opposite to

364 changes in prevalence of beech-hardwood forest. Hence, most of the vegetation changes at Story Lake
365 during the Holocene can be characterized as a shift in prevalence between these two types. Both oak
366 forest/woodland and beech-hardwood forest decreased in concert with Euro-American settlement at 0.02
367 ka, but oak forest/woodland rebounds slightly in the most recent pollen sample at 2019 CE, suggesting
368 some recent reforestation.

369 *Open or cleared vegetation:* This late-Holocene-to-Anthropocene vegetation type is dominated by the
370 herbaceous taxa ragweed (beta = 0.46) and grass (beta = 0.13). Prominence of open or cleared vegetation
371 is low prior to Euro-American land-use intensification, with small peaks (0.17 gamma) at 2.5 ka BP. During
372 the Euro-American period, this vegetation type prevailed, with a 0.96 gamma at 0.01 ka BP.

373 **Fire History**

374 The macroscopic charcoal record at Story Lake has a low signal-to-noise ratio (mean SNI = 2.7), with few
375 individual peaks clearly distinguishable from the background trend (Fig. 5b). A SNI >3 is needed to
376 confidently detect discrete fire events (Kelly et al. 2011). Low SNI values may indicate fire regimes
377 characterized by high frequency but low severity fires, in which charcoal produced by individual fire events
378 does not differ substantially from background values (Kelly et al. 2011). Alternatively, low SNIs can be due
379 to low sampling resolution or high sediment mixing (Kelly et al. 2011), neither of which are likely at Story
380 Lake due to high and contiguous sampling resolution and because the linear sedimentation rates observed
381 (Fig. 2) are higher than the median and mean rates (0.076 cm yr^{-1} , $0.14 \text{ cm year}^{-1}$) for other kettle lakes in
382 eastern North America (Goring et al. 2012), implying less time-averaging and mixing. Therefore, here we
383 focus on variations in total charcoal accumulation rates (CHAR) at Story Lake and interpret CHAR as a
384 proxy for shifts in the overall prevalence of low-intensity fires in the Story Lake watershed.

385 Charcoal was found in every sample, so times with zero charcoal represent a break in sampling due to
386 core breaks and not a lack of charcoal in a sample (Fig. 5b). Total CHAR appears to have a quasi-cyclical

387 pattern in the middle Holocene (8.0 to 4.5 ka BP) with gradual rise and fall of CHAR over approximately
388 1000-year periods, ranging from 3 pieces $\text{cm}^{-2} \text{ yr}^{-1}$ to 56 pieces $\text{cm}^{-2} \text{ yr}^{-1}$ (Fig. 5b). From 4.4 ka to 3.3 ka
389 CHAR is high, with an average of 38 pieces $\text{cm}^{-2} \text{ yr}^{-1}$. CHAR steadily rises between 4.7 and 3.7 ka, reaching
390 a maximum of 94 pieces $\text{cm}^{-2} \text{ yr}^{-1}$ at 3.7 ka (Fig. 5). After 3.5 ka, CHAR remains low (average of 12 pieces
391 $\text{cm}^{-2} \text{ yr}^{-1}$), with particularly low values after 1.0 ka (average of 8 pieces $\text{cm}^{-2} \text{ yr}^{-1}$), until Euro-American land
392 clearance, when CHAR increases to an average of 20 pieces $\text{cm}^{-2} \text{ yr}^{-1}$ (Fig. 5).

393 **Hydroclimate History**

394 Lake levels and $\delta^{13}\text{C}_{\text{beech}}$ record different phenomena and so provide different perspectives on the
395 hydroclimate history of northern Indiana. The Lake Lavine reconstruction of past water level, which is
396 governed by the watershed-scale balance between precipitation and evapotranspiration, shows a general
397 increase in lake level over the Holocene, starting at 8.0 ka BP with a water depth 333 cm below modern
398 levels (Fig. 5d). This increase suggests a generally positive water balance across much of the Holocene
399 (Ray-Cozzens 2022). This trend was interrupted by several reversals, indicating periods of negative water
400 balance. The first period of lake level increase lasted from 7.2 ka BP to 6.7 ka BP, followed by a subsequent
401 decrease from 6.7 ka BP to 6.4 ka BP (Fig. 5d). There were three distinct periods of drought identified by
402 sharp but short-duration decreases in lake level at 5.7 ka BP, 5.1 ka BP, and 4.7 ka BP, plus three more
403 prolonged periods of lowered lake level from 6.4 to 6.0 ka BP, 3.9 to 3.5 ka, and 2.9 to 2.5 ka BP (Fig. 5d).

404 The values of $\delta^{13}\text{C}_{\text{beech}}$ at Story varies between -29.7 ‰ and -21.0 ‰ and thus indicate a fairly large range
405 of variation in the iWUE of beech trees around Story Lake during the past ~5,000 years (Fig. 5c). The mean
406 analytical range among individual aliquots from the same sample is 1.6‰. For most time periods $\delta^{13}\text{C}_{\text{beech}}$
407 values are highly negative, indicating low iWUE and prioritization of carbon gain over water loss. There
408 are brief periods of higher iWUE ($\delta^{13}\text{C}_{\text{beech}} > \text{mean } \delta^{13}\text{C}_{\text{beech}} [-25.1\text{‰}]$) at 4.8 ka BP, 4.4 ka BP, 3.3 ka BP, 2.9
409 ka BP, 2.7 ka BP, 2.6 to 2.4 ka BP, 1.7 to 1.6 ka BP, and 0.6 to modern (Fig. 5c), possibly indicating

410 prioritization of water conservation. The time series of $\delta^{13}\text{C}_{\text{beech}}$ at Story Lake shows both some similarities
411 to and differences from sub-regional hydroclimate changes deduced from water levels at nearby Lake
412 Lavine (Fig. 5d). For example, two periods of decreased water level at 5.1 and 4.7 ka BP are followed by
413 excursions towards more positive $\delta^{13}\text{C}_{\text{beech}}$ and higher iWUE at 4.8 and 4.4 ka BP (Fig. 5c, d), with a 300
414 year lag in iWUE for each event. If these proxies are recording the same events, the lags may result from
415 chronological uncertainties in both records, or may indicate a differential sensitivity or response time. The
416 records differ in that there are other periods when iWUE fluctuated but lake levels remained relatively
417 constant (e.g. after 2.0 ka BP). Moreover, $\delta^{13}\text{C}_{\text{beech}}$ and iWUE show no long-term increase (Fig. 5c), unlike
418 the long-term increase in lake levels during the past 5.0 ka BP (Fig. 5d).

419 **Correlations among Proxies**

420 Simple correlation relationships suggest a significant relationship between charcoal accumulation rates
421 (CHAR) and the abundances of both beech and oak pollen abundances (Fig. 6). CHAR shows a positive
422 correlation with oak abundance (slope = 37.0, p-value <0.001, r^2 = 0.11, Pearson's correlation = 0.33) and
423 a negative correlation with beech abundance (slope = -58.9, p-value < 0.001, r^2 = 0.14, Pearson's
424 correlation = -0.38) (Fig. 6). The 95th quantile regression shows an even stronger relationship between
425 CHAR and oak (slope = 76.8, p-value < 0.001) and CHAR and beech (slope = -152.1, p-value < 0.001),
426 suggesting that beech and oak abundances may be particularly sensitive to more intense fire regimes.

427 In contrast, there is no significant relationship between the relative abundance of beech pollen and
428 $\delta^{13}\text{C}_{\text{beech}}$ (p-value = 0.06, Fig. 7), although the Pearson's correlation (0.28) suggests a modestly positive
429 correspondence. Comparison of the $\delta^{13}\text{C}_{\text{beech}}$ and beech abundance time series shows possible evidence
430 that the correlational structure has shifted over time. For example, between 5.0 and 4.0 ka two positive
431 but single-point excursions of $\delta^{13}\text{C}_{\text{beech}}$ (higher iWUE) correspond to declines in beech abundance (Fig. 7).
432 Conversely, at 2.2 and 1.5 ka BP negative excursions in $\delta^{13}\text{C}_{\text{beech}}$ (lower iWUE) match declines in beech

433 abundance whereas a positive excursion in $\delta^{13}\text{C}_{\text{beech}}$ (higher iWUE) at 1.7 ka BP is associated with a peak
434 in beech abundance (Fig. 7).

435 **Relative timing of beech fluctuations at Story, Appleman, Pretty, and Spicer**

436 **Lakes**

437 Fluctuations of beech populations are synchronous at the landscape scale but asynchronous regionally
438 (Fig. 8). Two lakes located within 15 km of Story Lake, Appleman and Pretty Lakes, show positive
439 correlation with Story Lake (Pearson's correlation 0.79 and 0.66 respectively; Fig. 8), suggesting that the
440 rises and declines in beech populations recorded at Story Lake were part of broader vegetation
441 phenomena recorded across northeastern Indiana. Of these three sites, the Holocene record at Story Lake
442 is the best dated. Uncertainties in the Holocene age-depth models at Appleman and Pretty Lake are large
443 enough (Appleman) or confounded by hardwater effects (Pretty) that lead/lag relationships among these
444 records cannot be assessed (Supplemental Information). The number and timing of rapid change events
445 in beech are not correlated between Story Lake and Spicer Lake ($p\text{-value}=0.39$; Fig. 8). The age-depth
446 models for Story and Spicer Lakes records are well constrained, with 17 age controls at Story Lake and 17
447 age controls at Spicer Lake (Wang et al., 2016), and generally linear sedimentation rates at both sites. At
448 Spicer Lake, beech experienced three rapid but short-lived decreases (5.3 ka BP, 4.3 ka BP, and 1.2 ka BP)
449 and one rapid decrease followed by a prolonged period of low abundance (3.2 ka BP to 1.8 ka BP, Fig. 8)
450 (Wang et al. 2016). None of these rapid changes are apparent at Story Lake (Fig. 8). To test whether the
451 Story and Spicer records show synchronous events given age uncertainty, we identified three events that
452 could be plausibly correlated between the Story and Spicer records: the initial rise at ca. 7.5 ka and the
453 beginning and end of a prolonged period of low beech abundances during the middle to late Holocene
454 (Fig. 8, red points with whiskers). Initial expansion is similar (within 200 years) but not synchronous ($p\text{-}$
455 $\text{value} < 0.05$). For the middle-Holocene decline in beech abundances at Story Lake at 4.6 ka we identified

456 two possible matches at Spicer, at 4.2 ka BP and 3.2 ka BP (Fig. 8b). Although the pattern of the middle
457 Holocene beech low period is similar the timing of the onset of low beech at Story Lake (4.6 ka BP) and
458 both potential onsets at Spicer Lake (4.2 ka BP and 3.2 ka BP) are significantly different (p-value <0.05),
459 as is the timing of recovery (2.8 ka BP at Story Lake and 1.8 ka BP at Spicer Lake, p-value <0.05; Fig. 8).
460 These inter-site comparisons thus demonstrate apparent synchrony of beech dynamics at a landscape
461 scale (i.e. among sites in northeastern Indiana) and regional-scale asynchrony (i.e. between northwestern
462 and northeastern Indiana).

463 **Discussion**

464 **Shifts in sensitivity to fire and climate drivers of oak-beech transitions in the** 465 **Southern Great Lakes**

466 Multiple lines of evidence suggest that ecosystem-type conversions and the prevalence of mesic beech-
467 hardwood forests and oak forest/woodland at the northern margin of the former Prairie Peninsula were
468 closely regulated by shifts in fire regime and secondarily by hydroclimate and other factors. These
469 dynamics acted to synchronize beech fluctuations at local to landscape scales and produce asynchronous
470 changes at regional scales (northwest Indiana versus northeast Indiana). The positive and negative
471 feedbacks among hydroclimate, fire, and vegetation appear to have varied in strength and direction over
472 time (Fig. 9). Consequently, the ecoclimatic sensitivity of vegetation shifted over time, including periods
473 of relatively high sensitivity to extrinsic drivers and other periods where beech-hardwood forests
474 persisted despite strong extrinsic forcing.

475 *8.0 to 4.6 ka: High sensitivity to fire and climate (Fig. 9a)* - The initial expansion of beech-hardwood forests
476 in the Story Lake region between 7.3 and 7.1 ka was rapid, which is consistent with other sites in the
477 regions which show similar rapid expansions of beech upon arrival (Bennett 1988) and occurred during a
478 period of low fire prevalence and net positive water balance, as indicated by low CHAR and rising lake

479 levels (Fig. 5). The subsequent decline in beech-hardwood forests between 5.0 ka and 4.6 ka appears to
480 have been largely governed by disturbance regime and extrinsic climatic factors, because the decline
481 corresponds closely to an intensifying fire regime (as indicated by a rise in CHAR beginning at 6.0 ka, Fig.
482 5b) and brief periods of increased iWUE and likely water stress in beech (Fig. 5c). During this period of
483 beech-hardwood forest declines, the individual fluctuations in total CHAR show no clear connection to
484 fluctuations in vegetation prevalence. Rather, the multi-centennial decline in beech-hardwood forests is
485 matched by a multi-centennial increase in fire activity.

486 Coincident with the increase in fire activity, Mg/Ca data from Lake Geneva on the Wisconsin-Illinois border
487 indicate potential regional warming from 5.2-4.6 ka, with high temperatures then persisting until 3.8 ka
488 (Puleo et al., 2020). The warming would be expected in Indiana as part of a large-scale change in
489 atmospheric patterning reconstructed in the northeast U.S. (Shuman et al., 2023). If this temperature
490 record applies regionally, the warming may explain the increased fire activity, even though the Lake Lavine
491 water levels increased substantially from 5.0 to 4.4 ka BP. Both fire and warming could have worked in
492 concert to reduce beech-hardwood forests, while favoring oak-derived fuels conducive to increased
493 wildfire. Oak and beech have differing temperature preferences; just as beech populations extended
494 further north historically into Michigan than oak (Fig. 1), oak pollen abundances peak today where mean
495 July temperatures exceed 20°C whereas beech abundance peaks below 20°C (Williams et al., 2006). The
496 lake-level and charcoal records further suggest that effective moisture availability declined during and
497 preceding periods of intensified fire regime and increased iWUE (and possibly water stress) of beech, for
498 example at 5.2-5.0 ka BP and 4.9-4.6 ka BP (Fig. 5b-d). Hence, for this initial period (8.0 to 4.6 ka), one
499 hypothesis is that climate variations were the primary determinant of fire regime and thus also of
500 beech/oak prevalence (Fig. 9).

501 4.6 to 3.7 ka: Strong fire-vegetation coupling (Fig. 9b) - The period from 4.6 ka BP to 3.7 ka BP is marked
502 by prominence of oak forest/woodland, an active fire regime, potentially high regional temperatures, and

503 an initial increase but then stable or slightly declining lake levels (Fig. 5). The iWUE of beech appears to
504 be moderate to low (Fig. 5c), suggesting low moisture stress. Hence, during this period, a positive feedback
505 loop between fire-tolerant oak and a high-frequency but low-intensity fire regime may have been the
506 primary factor governing the dominance of oak forest/woodland and scarcity of mesic beech-hardwood
507 forests. Fire as an agent of maintaining prairie and oak woodland type ecosystems has been widely seen
508 during the Holocene in the eastern Prairie Peninsula and eastern US (Nelson et al. 2006, Vose and Elliot
509 2016, Nowacki and Abrams 2008). Many oak species are particularly well adapted to frequent low
510 intensity fire regimes due to their thick bark, suitability of fire disturbed landscapes for seeding, ability to
511 resprout after fire, deep root systems, and suppression of fire sensitive competitors (Vose and Elliot 2016,
512 Abrams 1992). Therefore, frequent low intensity fires can promote establishment and spread of oak
513 woodlands through suppression of fire-intolerant species (e.g., beech), which could modify the understory
514 to suppress fires (Nowacki and Abrams 2008). Therefore, a prolonged period of oak woodland dominance
515 could have facilitated a positive feedback loop (Fig. 9) that supported the increased and sustained low
516 intensity fire regime at Story Lake from 4.6 ka BP to 3.4 ka BP, even during periods when $\delta^{13}\text{C}_{\text{beech}}$ and
517 iWUE suggests low water stress (Fig. 5). Notably, a peak in beech abundance at 4.0 ka BP when beech
518 pollen accumulation rates equal those at other times of beech dominance (Supplemental Information)
519 may have been limited by wildfire at Story, in contrast to Spicer where fire was limited and beech
520 abundance was high until 3.2 ka BP (Fig. 8).

521 3.7 to 2.8 ka: Rapid ecosystem transition linked to shifting fire and climate (Fig. 9c) - After 3.7 ka BP, fire
522 activity sharply declines until a low point at 3.2 ka BP (Fig. 5b), which coincides with increased water
523 availability and decreased iWUE (Fig. 5). These relationships suggest a direct regulation of fire regime by
524 climate, which is consistent with current controls on wildfire in the Great Lakes Region where winter and
525 early spring precipitation and snow cover are major controls over fire frequency and thus the presence of
526 mesic, fire intolerant forests (Henne et al. 2007, Cardille et al. 2001). Late summer precipitation is also an

527 important deterrent for wildfire in the Great Lakes region (Cardille et al. 2001). However, $\delta^{18}\text{O}$ Holocene
528 records in northeastern Indiana, southeastern Wisconsin, and eastern North America indicate no change
529 in precipitation seasonality (Stuiver 1968, Puleo et al. 2020, Stefanescu et al. 2023); therefore a
530 combination on increased summer and winter precipitation may have resulted in the decreased fire
531 regime seen at Story Lake. Regional cooling at 3.8-3.2 ka BP may have also been a factor (Puleo et al.,
532 2020; Shuman et al., 2023). Based on inferred changes in the latitudinal temperature gradient in eastern
533 North America, the warmest conditions would have been expected from 4.8-3.8 ka BP when oak-hickory
534 communities replaced cool-tolerant hardwood forests in Pennsylvania, New York, and Massachusetts
535 (Shuman et al., 2023) and the Mg/Ca ratio peaked in southern Wisconsin (Puleo et al., 2020). Today,
536 climate patterns show that cool north-central areas of North America tend to decrease wildfire activity;
537 temperature has a strong influence on wildfire activity via vapor-pressure deficits and effects on fuel
538 moisture (Gedalof, 2010).

539 An increase of hickory at 3.6 ka (Fig. 3) suggests that the climate changes and diminished fire resulted first
540 in in-filling of oak woodlands and establishment of oak-hickory forests. Then, 400 years after the decline
541 of fire, mesic beech-hardwood forests rapidly increase in prevalence at 2.8 ka BP. This sequence thus
542 could suggest a prolonged two-stage successional change that is obscured by the lack of species-level
543 resolution for many pollen taxa, particularly oak. For example, a plausible infilling of oak woodlands to
544 oak forests and shift from more fire-tolerant (e.g. *Q. macrocarpa*, *Q. alba*, *Q. ellipsoidalis*) to fire-sensitive
545 oak species (e.g. *Q. velutina*, *Q. rubra*) that cannot be differentiated by pollen analysis. Alternatively,
546 regional temperatures, a factor not captured at Story Lake, may have continued to decline until 2.9 ka
547 (Shuman et al., 2023). The continued cooling thus could have directly or indirectly affected the ability of
548 mesic beech-hardwood forests to outcompete oak forest/woodland and would explain why oak remained
549 dominant until 2.8 ka BP, even though fire activity declined after 3.7 ka BP.

550 The differences between beech histories at Spicer and Story (Fig. 8) argue somewhat against strong direct
551 regulation by temperature, because temperature variations tend to be spatially autocorrelated at
552 landscape to regional scales. However, prior work in Minnesota's Big Woods indicates that regional-scale
553 temperature variations, combined with local- to landscape variations in fire exposure and moisture
554 availability, can produce a spatial and temporal mosaic of rapid vegetation changes (Shuman et al. 2009,
555 Umbanhowe 2004). Additionally, an increase in winter precipitation between 7.0 ka BP and 4.0 ka BP is
556 observed in western Michigan, at sites immediately downwind of Lake Michigan, suggesting localized lake-
557 effect snow (Henne and Hu 2010), which could be a factor in the difference between Story and Spice Lake
558 to the west. The proximity of Spicer Lake to Lake Michigan (Fig. 1) may have made it more subject to lake
559 effects and hence differing Holocene variations in temperatures, moisture, and fire history than the
560 northeastern sites (Story, Appleman, and Pretty, Fig. 8).

561 With or without a direct temperature influence, the rapid ecosystem transition at 2.8 ka (Fig. 4, 5a)
562 involved a first-stage establishment of nearly fire-free oak-hickory forests that allowed beech and other
563 fire-sensitive hardwoods, such as maple, to establish in the understory and later become widely prevalent.
564 The lag time between cessation of fire regime and the rapid establishment of beech forests is
565 approximately 400 years, suggesting that some abrupt ecosystem transitions may occur centuries after
566 the original triggering event. A positive feedback loop between increasing beech abundance and
567 establishment of microclimates inimical to fire establishment and spread may have further accelerated
568 this transition (Nowacki and Abrams 2008, Alexander et al. 2021). The low beech iWUE during this
569 transition (Fig. 5c), suggests that the combination of high-water availability and suppressed fire regime
570 may be essential for enabling this rapid ecosystem transition (Fig. 9).

571 *2.8 ka to European Settlement: Vegetation Persistence and Stable State (Fig. 9d)* - After 2.8 ka, the
572 prevalence of oak forest/woodland and beech-hardwood forests around Story Lake fluctuated but
573 remained roughly even on the landscape from 2.8 ka until the onset of Euro-American land clearance

574 (1860 CE), despite large fluctuations in $\delta^{13}\text{C}_{\text{beech}}$ (Fig. 5). Moreover, the Lake Lavine record suggests a
575 period of lowered lake levels between 3.0 and 2.5 ka, soon after the rapid re-establishment of mesic
576 beech-hardwood forests without re-establishment of oak forest/woodland dominance. This vegetation
577 persistence despite ongoing hydroclimate variability suggests that a new stable state had been reached
578 in which beech is maintained internally through a stabilizing negative feedback loop that is resilient to
579 hydroclimate variability (Fig 9). In this negative feedback loop, high beech abundances create
580 microclimates favorable to beech recruitment and inimical to fire spread, thus reducing ecosystem
581 sensitivity to environmental variability (Nowacki and Abrams 2008, Alexander et al. 2021). Nonetheless,
582 some of the brief excursions in prevalence of oak forest/woodland and beech-hardwood forest may be
583 linked to hydroclimate perturbations or to small shifts in fire regime (Fig. 5b), or to intrinsic ecosystem
584 processes such as frequency dependent species interactions (Ramiadantsoa et al. 2019). Overall, we
585 hypothesize that the persistence of beech-hardwood forest during the late Holocene, prior to Euro-
586 American arrival is primarily governed by intrinsic processes and stabilizing vegetation feedbacks (Fig. 9).

587 **Other possible drivers not directly analyzed**

588 In addition to internal ecosystem processes and climate, humans may have also affected fire and
589 vegetation dynamics at Story Lake, although human activities are not directly captured in our proxy
590 network. Archaeological records from the middle Holocene suggest that human societies in Indiana were
591 highly mobile foragers, although the population and community dynamics of peoples in this time-period
592 and region are not well understood (Stafford et al. 2000, Jones and Johnson 2016). Summed probabilities
593 for calibrated radiocarbon dates from archaeological contexts in the Great Lake Region (calculated from
594 Kelly et al. 2022 using the method in Surovell et al. 2009), which are often used as a simple indicator of
595 human population abundances, suggests a population increase from 6.5 ka BP to 5.5 ka BP, then a period
596 of low population from 5.5 ka KP to 3.9 ka BP, and a gradual increase from 3.9 ka BP to a peak at 0.7 ka
597 BP. These fluctuations in radiocarbon date summed probabilities do not appear to correspond to changes

598 in fire intensity, which peaks from 4.4 ka BP to 3.7 ka BP during a low point of human population. The
599 rapid beech increase at 2.9 ka BP occurs during the middle of the population increase, but at a point when
600 population is still low. Native American communities at other sites in the Upper Midwest and
601 Northeastern US have managed landscapes using fire (Abrams and Nowacki 2019, Abrams and Nowacki
602 2008, Clark and Royall 1996), likely with localized and patchy impacts (Munoz et al., 2014). Many late-
603 Holocene pollen records in eastern North America do not have clear signals of human activity (Gajewski
604 et al. 2019). To further elucidate the effects of human societies and environmental change on ecosystem
605 dynamics in the Great Lakes region, more work is needed with paired pollen, charcoal, and hydroclimate
606 proxies at sites with known human occupation, as has been done in Ontario (Munoz and Gajewski 2010,
607 McAndrews and Boyko-Diakonow 1989, Burden et al. 1986).

608 Pests and pathogens have also been invoked as possible mechanisms for rapid declines in tree populations
609 during the Holocene. Hemlock looper outbreaks have been suggested as a cause for the eastern hemlock
610 declines (Davis, 1981, Bhiry and Filion 1996, Booth et al. 2012a), but other studies have failed to find
611 evidence of looper outbreaks (Oswald et al. 2017). Beech is a thin-barked species that has been highly
612 susceptible to the introduction of the beech scale insect (*Cryptococcus fagisuga*) from Europe in the 1890s
613 and the outbreak of beech bark disease, which arises from the infection of various fungal species after
614 beech scale insect infestation (Beckman et al. 2021). Modern studies on European beech (*Fagus sylvatica*)
615 have found that stands are susceptible to pathogen damage, such as from the fungus *Kretzschmaria*
616 *deusta*, which has been found in beech forests during the Holocene, with high abundances of fungal
617 ascospores traced to flood events (van Geel et al. 2013, Cordin et al. 2021). However, pests and pathogens
618 are difficult to detect using traditional palaeoecological approaches, such that even in ecosystems with
619 regular insect outbreaks (e.g. bark beetles), the outbreaks can only be detected through indirect means
620 (Morris and Brunelle, 2012) or at small forest hollow sites (Schafstall et al. 2020). Hence, whether pests

621 and pathogens had any effect on American beech dynamics during the Holocene remains possible but
622 unknown and unstudied.

623 **Interpreting and reconciling the $\delta^{13}\text{C}_{\text{pollen}}$ record**

624 Much of the insight gained in this study into past fire-climate-vegetation interactions comes from having
625 multiple proxies from the same core, with precise relative depth positioning. In particular, the analysis of
626 $\delta^{13}\text{C}_{\text{beech}}$ enables a more direct understanding of whether beech water use responds to changes in water
627 balance (from lake level proxies) and whether those responses scale to changes in beech population
628 abundance. Several prior studies have shown a positive correlation between $\delta^{13}\text{C}_{\text{pollen}}$ and drought stress
629 for many plant species including *Cedrus* (Bell et al. 2017), *Nothofagus* (Griener et al. 2013), *Artemisia*, and
630 *Ambrosia* (Nelson et al. 2012). Other studies have shown that Holocene shifts in vegetation in eastern and
631 midwestern North America are linked to past hydroclimate variations, e.g. the mid-Holocene abrupt
632 declines of hemlock (Booth et al. 2012a, Shuman 2012, Marsicek et al. 2013), mid- to late-Holocene
633 declines in beech (Booth et al. 2012b, Wang et al. 2016), and shifts in the prairie-forest ecotone (Nelson
634 et al. 2006, Williams et al. 2010). Most of these studies have paired fossil pollen records with paleoclimatic
635 proxies that are sourced from lacustrine or palustrine archives (Clifford and Booth 2015, Shuman et al.
636 2009). However, trees, lakes, and bogs have different sensitivities to hydroclimate fluctuations, with
637 differently scaled integrations across watershed ecohydrology and different response times to
638 atmospheric shifts in water supply and demand. Therefore, even paleo-hydrological proxies from the
639 same sediment cores as fossil pollen or paired well-dated sites may not provide a direct measure of plant
640 responses to changes in hydroclimate. This differential response of proxies to changing water availability
641 has hampered understanding of the direct vegetation response to changes in hydroclimate.

642 The analyses here generally suggest some correspondences between the hydrological water balance at
643 Lake Lavine (Fig. 5d) and iWUE of beech at Story Lake (Fig. 5c), but also notable differences. Some

644 individual events appear to correlate drought periods with high iWUE and high beech abundance, e.g. at
645 5.1 ka BP and 4.7 ka BP, while others periods show the opposite pattern with no apparent correlation
646 between moisture availability, iWUE, and beech abundance, e.g. after 2.4 ka BP. However, small
647 fluctuations in lake level may not be apparent in the lake level reconstruction due to low sampling in
648 shallow cores. Additionally, the long-term wetting trend from 8.0 ka BP to present in the lake level
649 reconstruction is not apparent in $\delta^{13}\text{C}_{\text{beech}}$. One possible explanation is that biological systems are often
650 characterized by homeostatic mechanisms, while physical hydrological systems might or might not.
651 Hence, the ratio of photosynthesis to stomatal conductance is only expected to vary within physiological
652 limits that prevent the $\delta^{13}\text{C}$ values of C_3 plants from becoming too positive or negative. It is also possible
653 that there is intraspecific variation in iWUE among beech trees and successional dynamics across the
654 lifetime of individual trees may favor individuals with generally higher or lower iWUE, thus acting to
655 stabilize population-level shifts in iWUE inferred from $\delta^{13}\text{C}_{\text{beech}}$ across centennial-millennial scales.
656 Conversely, if atmospheric annual water balance is positive, lake water level should continue to increase,
657 until water levels are high enough that a stream outlet or other balancing outflow is reached. Therefore,
658 a one-to-one relationship between pollen $\delta^{13}\text{C}$ values and lake levels is not to be expected.

659 The absence of a significant relationship $\delta^{13}\text{C}_{\text{beech}}$ and beech abundance at Story Lake (Fig. 7) is surprising
660 given that a positive correlation between $\delta^{13}\text{C}$ and drought stress is reported in modern studies of various
661 taxa (Bell et al. 2017, Griener et al. 2013, Nelson et al. 2012). As explained above, one hypothesis for this
662 lack of a relationship is that water availability is the main regulator of $\delta^{13}\text{C}$, but that, as fire-climate-
663 vegetation feedbacks shift in strength and direction over time, water availability is a secondary and
664 intermittent regulator of beech population abundances, with periods of direct hydroclimate control on
665 beech populations and periods of indirect regulation though mediating fire regimes (Fig. 9). Alternatively,
666 variations $\delta^{13}\text{C}_{\text{beech}}$ and iWUE during the Holocene might be affected by other factors beyond moisture
667 availability. For example, increased photosynthesis has been a major driver of increased iWUE in response

668 to increased atmospheric CO₂ during the past century (Mathias and Thomas, 2021); however, during the
669 Holocene, the effects of CO₂ on iWUE should be muted, given that atmospheric CO₂ variations were
670 modest, with a linear rise of only 260 to 280 ppm between 8.2 ka and 1800 CE (Indermuhle et al., 1999).
671 Changes in temperature during the Holocene (Shuman et al. 2023) may have also influenced iWUE
672 through the influence of temperature on photosynthesis (Dusenge et al. 2018), potentially interacting
673 with changes in water availability.

674 **Landscape to regional controls on beech declines and beech-oak dynamics**

675 The multiple rapid beech fluctuations throughout the Holocene in northern Indiana appear to be
676 synchronous at the landscape scale (less than 15 km distance between Story, Appleman, and Pretty Lakes)
677 but are clearly asynchronous at regional scale (120 km distance between Story and Spicer Lakes). This
678 pattern of landscape-scale synchrony and regional asynchrony suggests that local- to landscape-scale
679 interactions between species, fire regime, and climate are the dominant drivers of vegetation change,
680 including rapid vegetation change (Fig. 9). Note also that Story Lake shows a close correspondence
681 between fire regime and vegetation dynamics (Figs. 5, 7) whereas Spicer Lake has little to no charcoal and
682 no clear correspondence between fire regime and vegetation change (Wang et al., 2016). Hence, the
683 importance of fire-vegetation feedbacks appear to vary intra-regionally, with fire an important driver of
684 ecological change at Story Lake and generally unimportant at Spicer Lake.

685 Within-landscape correlations among sites in beech abundance (within 15 km) suggests that small scale
686 factors, such as disturbance, have a local synchronizing effect in northern Indiana. Although proxies for
687 fire and water stress were not collected at Appleman or Pretty lakes, the synchrony between sites
688 suggests that the same factors are driving vegetation change at all local sites. Therefore, the interactions
689 between fire and hydroclimate that are seen at Story Lake are likely important at all three sites. The
690 controlling effects of fire on forest transitions are well documented during the Holocene such as the

691 prairie peninsula (Nelson et al. 2006, Nelson and Hu 2008), Minnesota's big woods (Calder 2016,
692 Umbanhower 2004, Shuman et al. 2009), and eastern North America (Abrams and Nowacki 2019).

693 Intra-regional differences in hydroclimate and vegetation dynamics might also be governed by the lake-
694 effect snow, which intensifies local hydroclimate variability (Booth et al., 2012b) and has been shown to
695 affect vegetation composition in Michigan (Henne et al. 2007). Spicer Lake, which is 17 km from the
696 southeastern shore of Lake Michigan, may be more affected by variations in lake-effect snow, while Story
697 Lake, further east, may be more directly regulated by past shifts in fire regime. This lake-effect hypothesis
698 is consistent with the pre-settlement distribution of beech which positively correlated with total snowfall
699 (Seely et al. 2019) with the importance of lake-effect snow in maintaining snow cover throughout the
700 winter being especially important in areas with coarse textured soils which do not retain water and rely
701 on snowmelt for establishment of mesic species in the spring (Henne et al. 2007). This is also seen during
702 the MCA, where both droughts and beech declines were heterogenous on the landscape with sites that
703 had more pronounced drought also having larger beech declines (Booth et al., 2012b). Hence, just as the
704 importance and directionality of fire, vegetation, and climate interactions at Story Lake appears to vary
705 during the Holocene (Figs. 5, 9), the relative importance of these drivers and interactions likely varied
706 spatially as well, across all scales considered here: local, landscape, and regional.

707 Additional multi-proxy and high-resolution records are needed to further disentangle the interacting
708 effects of climate, fire, and vegetation dynamics at local to sub-regional scales. Further insight can be
709 gained also by more advanced statistical analyses than the relatively simple correlational analyses shown
710 here. In particular, advances in ecological modeling, such as state-space models, allow more precise
711 testing of hypotheses about drivers of community dynamics and allow separation of process-based drivers
712 from observational errors inherent in palaeoecological data e.g., time uncertainty and sampling errors
713 (Auger-Méthé et al. 2021). Combining a large network of multi-proxy high-resolution sites with state-
714 space models can provide further quantification of regional drivers of ecological change.

715 **Conclusions**

716 The interacting effects of fire and climate on ecosystem-type conversions is a major societal concern and
717 the beech-oak mosaic in northern Indiana offers a useful model system for understanding how these
718 changes in mesic forests are governed by past shifts in climate variability and fire regime. At Story Lake,
719 variations in the prevalence of beech-hardwood forests and oak forests/woodlands throughout the
720 Holocene, including rapid changes, are mediated by multiple and shifting feedbacks among climate, fire,
721 and vegetation. At Story Lake, fire appears to a strong regulator of vegetation composition changes, with
722 climate also exerting direct effects on fire regime and vegetation dynamics. Temperature variations may
723 also have played a role, a critical need is more independent paleotemperature proxies in this region.
724 Possible contributing factors that are mostly unexplored here include human activity and pests or
725 pathogens. The timing of beech declines differs from those observed at Spicer Lake, where fire is not
726 prevalent, suggesting that variation in local fire regime (and perhaps also moisture availability via lake-
727 effect snow) drives intraregional differences in beech population dynamics. This work has shown the
728 potential for $\delta^{13}\text{C}_{\text{beech}}$ in assessing both the sensitivity of beech to hydroclimate perturbations and
729 identifying periods of beech forest persistence despite apparently large changes in iWUE and moisture
730 availability. These periods of persistence may indicate strong stabilizing feedbacks.

731 Climate change is one of the main threats to American beech and, in Indiana, climates are expected to get
732 warmer and wetter with more extreme events and less snowfall (Beckman et al. 2021, Widhalm et al.
733 2018). With beech bark disease now introduced and fire events mostly suppressed, the interactions
734 between climate variability, disturbance regime, and disease are likely to be very different between the
735 Holocene dynamics studied here and those of the 21st century. Nonetheless, fire-climate feedbacks are
736 an underappreciated source of risk in the Great Lakes region, and rising temperatures and future drought
737 events may have profound effects on beech populations in the Great Lakes region through initiating more

738 fires and favoring oak forests over beech forests as seen at Story Lake during the Holocene.

739 Recommendations for future work include 1) the continued building of a high-resolution multi-proxy

740 network to further disentangle the interacting effects between vegetation, fire regime, climate, and

741 human activity, 2) furthering our understanding of the behavior of $\delta^{13}\text{C}$ (e.g. through paired high-

742 resolution $\delta^{13}\text{C}$ analyses of pollen grains from lake sediments and tree rings of the same taxa) to

743 disentangle stand- and landscape level signals of tree physiological reactions to changes in water

744 availability; 3) the development and application of state-space modeling approaches to further establish

745 causality of vegetation change within and across networks of sites at local to subcontinental scales, and

746 4) conducting forward looking studies to better understand how climate change, disturbance regime, and

747 pathogens may impact feedbacks between climate, fire, and vegetation in the Great Lakes region which

748 will both advance our understanding of the underlying fundamental processes and help direct future

749 conservation efforts.

750 **References**

751 Abrams, M., Downs, J., 2011. Successional Replacement of Old-Growth White Oak by Mixed-Mesophytic
752 Hardwoods in Southwest Pennsylvania. *Canadian Journal of Forest Research* 20, 1864–1870.
753 <https://doi.org/10.1139/x90-250>

754 Abrams, M.D., 1992. Fire and the Development of Oak Forests. *BioScience* 42, 346–353.
755 <https://doi.org/10.2307/1311781>

756 Adams, K.D., Negrini, R.M., Cook, E.R., Rajagopal, S., 2015. Annually resolved late Holocene
757 paleohydrology of the southern Sierra Nevada and Tulare Lake, California. *Water Resources
758 Research* 51, 9708–9724. <https://doi.org/10.1002/2015WR017850>

759 Alexander, H.D., Siegert, C., Brewer, J.S., Kreye, J., Lashley, M.A., McDaniel, J.K., Paulson, A.K.,
760 Renninger, H.J., Varner, J.M., 2021. Mesophication of Oak Landscapes: Evidence, Knowledge
761 Gaps, and Future Research. *BioScience* 71, 531–542. <https://doi.org/10.1093/biosci/biaa169>

762 Allen, C.D., Breshears, D.D., McDowell, N.G., 2015. On underestimation of global vulnerability to tree
763 mortality and forest die-off from hotter drought in the Anthropocene. *Ecosphere* 6, art129.
764 <https://doi.org/10.1890/ES15-00203.1>

765 Auger-Méthé, M., Newman, K., Cole, D., Empacher, F., Gryba, R., King, A.A., Leos-Barajas, V., Mills
766 Flemming, J., Nielsen, A., Petris, G., Thomas, L., 2021. A guide to state-space modeling of
767 ecological time series. *Ecological Monographs* 91, e01470. <https://doi.org/10.1002/ecm.1470>

768 Bacon, M., 2009. Water use efficiency in plant biology. John Wiley & Sons.

769 Beckman, E., Meyer, A., Pivorunas, D., Hoban, S., and Westwood, M., 2021. Conservation Gap Analysis of
770 American Beech. Lisle, IL: The Morton Arboretum.

771 Belmecheri, S., Maxwell, R.S., Taylor, A.H., Davis, K.J., Freeman, K.H., Munger, W.J., 2014. Tree-ring δ13C
772 tracks flux tower ecosystem productivity estimates in a NE temperate forest. *Environ. Res. Lett.*
773 9, 074011. <https://doi.org/10.1088/1748-9326/9/7/074011>

774 Bennett, K.D., 1985. The Spread of *Fagus grandifolia* Across Eastern North America During the Last 18
775 000 years. *Journal of Biogeography* 12, 147–164. <https://doi.org/10.2307/2844838>

776 Bennett, K.D., 1988. Holocene Geographic Spread and Population Expansion of *Fagus Grandifolia* in
777 Ontario, Canada. *Journal of Ecology* 76, 547–557. <https://doi.org/10.2307/2260612>

778 Bennett, K.D., 1987. Holocene history of forest trees in southern Ontario. *Can. J. Bot.* 65, 1792–1801.
779 <https://doi.org/10.1139/b87-248>

780 Bernabo, J.C., Webb, T., 1977. Changing patterns in the Holocene pollen record of northeastern North
781 America: A mapped summary. *Quaternary Research* 8, 64–96. [https://doi.org/10.1016/0033-5894\(77\)90057-6](https://doi.org/10.1016/0033-5894(77)90057-6)

782

783 Bhiry, N., Filion, L., 1996. Mid-Holocene Hemlock Decline in Eastern North America Linked with
784 Phytophagous Insect Activity. *Quaternary Research* 45, 312–320.
785 <https://doi.org/10.1006/qres.1996.0032>

786 Blei, D., Lafferty, J., 2006. Correlated topic models. *Advances in neural information processing systems*
787 18, 147.

788 Blei, D.M., 2012. Probabilistic topic models. *Commun. ACM* 55, 77–84.
789 <https://doi.org/10.1145/2133806.2133826>

790 Blei, D.M., Ng, A.Y., Jordan, M.I., 2003. Latent dirichlet allocation. *Journal of machine Learning research*
791 3, 993–1022.

792 Booth, R.K., 2008. Testate amoebae as proxies for mean annual water-table depth in Sphagnum-
793 dominated peatlands of North America. *Journal of Quaternary Science* 23, 43–57.
794 <https://doi.org/10.1002/jqs.1114>

795 Booth, R.K., Brewer, S., Blaauw, M., Minckley, T.A., Jackson, S.T., 2012a. Decomposing the mid-Holocene
796 Tsuga decline in eastern North America. *Ecology* 93, 1841–1852.

797 Booth, R.K., Jackson, S.T., Sousa, V.A., Sullivan, M.E., Minckley, T.A., Clifford, M.J., 2012b. Multi-decadal
798 drought and amplified moisture variability drove rapid forest community change in a humid
799 region. *Ecology* 93, 219–226. <https://doi.org/10.1890/11-1068.1>

800 Burden, E.T., McAndrews, J.H., Norris, G., 1986. Palynology of Indian and European forest clearance and
801 farming in lake sediment cores from Awenda Provincial Park, Ontario. *Can. J. Earth Sci.* 23, 43–
802 54. <https://doi.org/10.1139/e86-005>

803 Calder, W. J. (2016). *Interactions Among Climate Change, Wildfire, and Vegetation Shaping Landscapes
804 for the Last 2000 Years*. University of Wyoming, Ph.D. dissertation.

805 Cardille, J.A., Ventura, S.J., Turner, M.G., 2001. Environmental and Social Factors Influencing Wildfires in
806 the Upper Midwest, United States. *Ecological Applications* 11, 111–127.
807 <https://doi.org/10.2307/3061060>

808 Christensen, E.M., Harris, D.J., Ernest, S.K.M., 2018. Long-term community change through multiple
809 rapid transitions in a desert rodent community. *Ecology* 99, 1523–1529.
810 <https://doi.org/10.1002/ecy.2373>

811 Clark, J.S., Royall, P.D., 1996. Local and Regional Sediment Charcoal Evidence for Fire Regimes in
812 Presettlement North-Eastern North America. *Journal of Ecology* 84, 365–382.
813 <https://doi.org/10.2307/2261199>

814 Clifford, M.J., Booth, R.K., 2015. Late-Holocene drought and fire drove a widespread change in forest
815 community composition in eastern North America. *The Holocene* 25, 1102–1110.
816 <https://doi.org/10.1177/0959683615580182>

817 Cordin, G., Messina, G., Maresi, G., Zottele, F., Ferretti, F., Montecchio, L., Oliveira Longa, C., 2021.
818 *Kretzschmaria deusta*, a limiting factor for survival and safety of veteran beech trees in Trentino
819 (Alps, Northern Italy). *iForest* 14, 576–581. <https://doi.org/10.3832/ifor3830-014>

820 Davis, M.B., 1981. Quaternary History and the Stability of Forest Communities, in: West, D.C., Shugart,
821 H.H., Botkin, D.B. (Eds.), *Forest Succession: Concepts and Application*, Springer Advanced Texts
822 in Life Sciences. Springer, New York, NY, pp. 132–153. https://doi.org/10.1007/978-1-4612-5950-3_10

823 Davis, M.B., 1981. Outbreaks of forest pathogens in Quaternary history, in: Bharadwaj, D.C. (Ed.),
824 Proceedings of the Fourth International Palynological Conference. Birbal Sahni Institute of
825 Palaeobotany, Lucknow, India, pp. 216-227.

826 Davis, M.B., 1963. On the theory of pollen analysis. *American Journal of Science* 261, 897–912.
827 <https://doi.org/10.2475/ajs.261.10.897>

828 DenUyl, D., 1953. Indiana's old growth forests. *Proceedings of the Indiana Academy of Science* 63, 73–
829 79.

830 Digerfeldt, G., Almendinger, J.E., Björck, S., 1992. Reconstruction of past lake levels and their relation to
831 groundwater hydrology in the Parkers Prairie sandplain, west-central Minnesota.
832 *Palaeogeography, Palaeoclimatology, Palaeoecology* 94, 99–118. [https://doi.org/10.1016/0031-0182\(92\)90115-L](https://doi.org/10.1016/0031-0182(92)90115-L)

833 Dusenge, M.E., Duarte, A.G., Way, D.A., 2019. Plant carbon metabolism and climate change: elevated
834 CO₂ and temperature impacts on photosynthesis, photorespiration and respiration. *New
835 Phytologist* 221, 32–49. <https://doi.org/10.1111/nph.15283>

836 Edwards, K.J., Fyfe, R.M., Jackson, S.T., 2017. The first 100 years of pollen analysis. *Nature Plants* 3, 1–4.
837 <https://doi.org/10.1038/nplants.2017.1>

838 Engstrom, R.T., Crawford, R.L., Baker, W.W., 1984. Breeding Bird Populations in Relation to Changing
839 Forest Structure following Fire Exclusion: A 15-Year Study. *The Wilson Bulletin* 96, 437–450.

842 Erdman, C., Emerson, J.W., 2008. bcp: An R Package for Performing a Bayesian Analysis of Change Point
843 Problems. *Journal of Statistical Software* 23, 1–13. <https://doi.org/10.18637/jss.v023.i03>

844 Faegri, K., Kaland, P.E., Krzywinski, K., 1989. *Textbook of Pollen Analysis*, 4th ed.

845 Farquhar, G.D., Sharkey, T.D., 1982. Stomatal conductance and photosynthesis. *Annual Review of Plant
846 Physiology*.

847 Farquhar, G.D., Ehleringer, J.R., Hubick, K.T., 1989. Carbon Isotope Discrimination and Photosynthesis.
848 *Annual Review of Plant Physiology and Plant Molecular Biology* 40, 503–537.
849 <https://doi.org/10.1146/annurev.pp.40.060189.002443>

850 Finsinger W., Bonnici I. (2022) - tapas: an R package to perform trend and peaks analysis.
851 <https://doi.org/10.5281/zenodo.6344463> and any non-default settings applied.

852 Fuller, J.L., Foster, D.R., McLachlan, J.S., Drake, N., 1998. Impact of Human Activity on Regional Forest
853 Composition and Dynamics in Central New England. *Ecosystems* 1, 76–95.
854 <https://doi.org/10.1007/s100219900007>

855 Gajewski, K., 1987. Climatic impacts on the vegetation of eastern North America during the past 2000
856 years. *Vegetatio* 68, 179–190. <https://doi.org/10.1007/BF00114719>

857 Gajewski, K., 2019. Environmental history of the northwestern Québec Treeline. *Quaternary Science
858 Reviews* 206, 29–43. <https://doi.org/10.1016/j.quascirev.2018.12.025>

859 Gedalof, Z. E. (2010). Climate and spatial patterns of wildfire in North America. In *The Landscape Ecology
860 of Fire* (pp. 89–115). Dordrecht: Springer Netherlands.

861 Gill, J.L., Williams, J.W., Jackson, S.T., Lininger, K.B., Robinson, G.S., 2009. Pleistocene Megafaunal
862 Collapse, Novel Plant Communities, and Enhanced Fire Regimes in North America. *Science* 326,
863 1100–1103. <https://doi.org/10.1126/science.1179504>

864 Goring, S., Williams, J., Blois, J., Jackson, S., Paciorek, C., Booth, R., Marlon, J., Blaauw, M., Christen, J.,
865 2012. Deposition times in the northeastern United States during the Holocene: establishing valid
866 priors for Bayesian age models. *Quaternary Science Reviews* 48, 54–60.

867 Gray, H., 1989. Quaternary geologic map of Indiana. *Miscellaneous Map* 49.

868 Griener, K.W., Nelson, D.M., Warny, S., 2013. Declining moisture availability on the Antarctic Peninsula
869 during the Late Eocene. *Palaeogeography, Palaeoclimatology, Palaeoecology* 383–384, 72–78.
870 <https://doi.org/10.1016/j.palaeo.2013.05.004>

871 Grimm, E.C., 1984. Fire and Other Factors Controlling the Big Woods Vegetation of Minnesota in the
872 Mid-Nineteenth Century. *Ecological Monographs* 54, 291–311. <https://doi.org/10.2307/1942499>

873 Grimm, E.C., 1983. Chronology and Dynamics of Vegetation Change in the Prairie-Woodland Region of
874 Southern Minnesota, U.S.A. *The New Phytologist* 93, 311–350.

875 Grimm, E.C., Maher, L.J., Nelson, D.M., 2009. The magnitude of error in conventional bulk-sediment
876 radiocarbon dates from central North America. *Quaternary Research* 72, 301–308.
877 <https://doi.org/10.1016/j.yqres.2009.05.006>

878 Grün, B., Hornik, K., 2011. topicmodels: An R Package for Fitting Topic Models. *Journal of Statistical
879 Software* 40, 1–30. <https://doi.org/doi:10.18637/jss.v040.i13>

880 Hartmann, H., Moura, C.F., Anderegg, W.R.L., Ruehr, N.K., Salmon, Y., Allen, C.D., Arndt, S.K., Breshears,
881 D.D., Davi, H., Galbraith, D., Ruthrof, K.X., Wunder, J., Adams, H.D., Bloemen, J., Cailleret, M.,
882 Cobb, R., Gessler, A., Grams, T.E.E., Jansen, S., Kautz, M., Lloret, F., O'Brien, M., 2018. Research
883 frontiers for improving our understanding of drought-induced tree and forest mortality. *New
884 Phytologist* 218, 15–28. <https://doi.org/10.1111/nph.15048>

885 Haslett, J., Parnell, A., 2008. A simple monotone process with application to radiocarbon-dated depth
886 chronologies. *Journal of the Royal Statistical Society: Series C (Applied Statistics)* 57, 399–418.
887 <https://doi.org/10.1111/j.1467-9876.2008.00623.x>

888 Henderson, N.R., Long, J.N., 1984. A Comparison of Stand Structure and Fire History in Two Black Oak
889 Woodlands in Northwestern Indiana. *Botanical Gazette* 145, 222–228.

890 Henne, P.D., Hu, F.S., Cleland, D.T., 2007. Lake-effect snow as the dominant control of mesic-forest
891 distribution in Michigan, USA. *Journal of Ecology* 95, 517–529. [https://doi.org/10.1111/j.1365-2745.2007.01220.x](https://doi.org/10.1111/j.1365-
892 2745.2007.01220.x)

893 Henne, P.D., Hu, F.S., 2010. Holocene climatic change and the development of the lake-effect snowbelt
894 in Michigan, USA. *Quaternary Science Reviews* 29, 940–951.
895 <https://doi.org/10.1016/j.quascirev.2009.12.014>

896 Higuera, P.E., Brubaker, L.B., Anderson, P.M., Hu, F.S., Brown, T.A., 2009. Vegetation mediated the
897 impacts of postglacial climate change on fire regimes in the south-central Brooks Range, Alaska.
898 *Ecological Monographs* 79, 201–219. <https://doi.org/10.1890/07-2019.1>

899 Higuera, P.E., Gavin, D.G., Bartlein, P.J., Hallett, D.J., Higuera, P.E., Gavin, D.G., Bartlein, P.J., Hallett, D.J.,
900 2010. Peak detection in sediment–charcoal records: impacts of alternative data analysis
901 methods on fire-history interpretations. *Int. J. Wildland Fire* 19, 996–1014.
902 <https://doi.org/10.1071/WF09134>

903 IDNR (2019) Story Lake Bathymetric DeKalb County. Available at: https://www.in.gov/dnr/fish-and-wildlife/files/depth/fw-Story_Lake_Bathymetric_DeKalb_County_July_2019.pdf (Accessed: 23 August 2023)

904

905

906 Indermühle, A., Monnin, E., Stauffer, B., Stocker, T.F., Wahlen, M., 2000. Atmospheric CO₂

907 concentration from 60 to 20 kyr BP from the Taylor Dome Ice Core, Antarctica. *Geophysical*

908 *Research Letters* 27, 735–738. <https://doi.org/10.1029/1999GL010960>

909 Juggins, S., 2022. *riojaPlot*: Stratigraphic diagrams in R. Available at: <https://github.com/nsj3/riojaPlot>

910 (Last updated: 1 December 2022)

911 Jahren, A.H., 2004. The carbon stable isotope composition of pollen. *Review of Palaeobotany and*

912 *Palynology* 132, 291–313. <https://doi.org/10.1016/j.revpalbo.2004.08.001>

913 Jones, J.R. and Johnson, A.L., 2016. Early Peoples of Indiana. Indiana Department of Natural Resources

914 Division of Historic Preservation and Archaeology.

915 Jones, E.A., Lang, C.E., Laird, N.F., 2022. The Contribution of Lake-Effect Snow to Annual Snowfall Totals

916 in the Vicinity of Lakes Erie, Michigan, and Ontario. *Frontiers in Water* 4.

917 Kapp, R.O., Davis, O.K., King, J.E., 2000. Ronald O. Kapp's Pollen and Spores.

918 Kelly, R.F., Higuera, P.E., Barrett, C.M., Hu, F.S., 2011. Short Paper: A signal-to-noise index to quantify

919 the potential for peak detection in sediment–charcoal records. *Quaternary Research* 75, 11–17.

920 <https://doi.org/10.1016/j.yqres.2010.07.011>

921 Kelly, R.L., Mackie, M.E., Robinson, E., Meyer, J., Berry, M., Boulanger, M., Codding, B.F., Freeman, J.,

922 Garland, C.J., Gingerich, J., Hard, R., Haug, J., Martindale, A., Meeks, S., Miller, M., Miller, S.,

923 Perttula, T., Railey, J.A., Reid, K., Scharlotta, I., Spangler, J., Thomas, D.H., Thompson, V., White,

924 A., 2022. A New Radiocarbon Database for the Lower 48 States. *American Antiquity* 87, 581–

925 590. <https://doi.org/10.1017/aaq.2021.157>

926 Korasidis, V.A., Wing, S.L., Nelson, D.M., Baczyński, A.A., 2022. Reworked pollen reduces apparent floral

927 change during the Paleocene-Eocene Thermal Maximum. *Geology* 50, 1398–1402.

928 <https://doi.org/10.1130/G50441.1>

929 Landfire (2020) Biophysical Setting Description and Quantitative Models, U.S. Department of Agriculture

930 and U.S. Department of the Interior. Available at: <https://www.landfire.gov/bps-models.php>

931 (Accessed: 24 March 2023)

932 Lindsey, A.A., Crankshaw, W.B., Qadir, S.A., 1965. Soil Relations and Distribution Map of the Vegetation

933 of Presettlement Indiana. *Botanical Gazette* 126, 155–163.

934 Loader, N.J., Hemming, D.L., 2004. The stable isotope analysis of pollen as an indicator of terrestrial
935 palaeoenvironmental change: a review of progress and recent developments. *Quaternary
936 Science Reviews, Isotopes in Quaternary Paleoenvironmental reconstruction* 23, 893–900.
937 <https://doi.org/10.1016/j.quascirev.2003.06.015>

938 Marsicek, J.P., Shuman, B., Brewer, S., Foster, D.R., Oswald, W.W., 2013. Moisture and temperature
939 changes associated with the mid-Holocene *Tsuga* decline in the northeastern United States.
940 *Quaternary Science Reviews* 80, 129–142. <https://doi.org/10.1016/j.quascirev.2013.09.001>

941 Mathias, J.M., Smith, K.R., Lantz, K.E., Allen, K.T., Wright, M.J., Sabet, A., Anderson-Teixeira, K.J.,
942 Thomas, R.B., 2023. Differences in leaf gas exchange strategies explain *Quercus rubra* and
943 *Liriodendron tulipifera* intrinsic water use efficiency responses to air pollution and climate
944 change. *Global Change Biology* 29, 3449–3462. <https://doi.org/10.1111/gcb.16673>

945 Mathias, J.M., Thomas, R.B., 2021. Global tree intrinsic water use efficiency is enhanced by increased
946 atmospheric CO₂ and modulated by climate and plant functional types. *Proceedings of the
947 National Academy of Sciences* 118, e2014286118. <https://doi.org/10.1073/pnas.2014286118>

948 McAndrews J.H., Boyko-Diakonow M., 1989. Pollen Analysis of Varved Sediment at Crawford Lake,
949 Ontario: Evidence of Indian and European Farming. *Quaternary Geology of Canada and
950 Greenland. Geological Survey of Canada, Geology of Canada* 1, 528–530.

951 McNab, W.H., Cleland, D.T., Freeouf, J.A., Jr., Keys, J.E., Nowacki, G.J., Carpenter, C.A., 2007. Description
952 of ecological subregions: sections of the conterminous United States. *General Technical Report
953 WO-76B* 76B, 1–82. <https://doi.org/10.2737/WO-GTR-76B>

954 Morris, J. L., and Brunelle, A., 2012. Pollen accumulation in lake sediments during historic spruce beetle
955 disturbances in subalpine forests of southern Utah, USA. *The Holocene*, 22(9), 961–974.
956 <https://doi.org/10.1177/0959683612437870>

957 Munoz, S.E., Gajewski, K., 2010. Distinguishing prehistoric human influence on late-Holocene forests in
958 southern Ontario, Canada. *The Holocene* 20, 967–981.
959 <https://doi.org/10.1177/0959683610362815>

960 Munoz, S.E., Schroeder, S., Fike, D.A., Williams, J.W., 2014. A record of sustained prehistoric and historic
961 land use from the Cahokia region, Illinois, USA. *Geology* 42, 499–502.
962 <https://doi.org/10.1130/G35541.1>

963 Nelson, D.M., 2012. Carbon isotopic composition of *Ambrosia* and *Artemisia* pollen: assessment of a C3-
964 plant paleophysiological indicator. *The New Phytologist* 195, 787–793.

965 Nelson, D.M., Hu, F.S., 2008. Patterns and drivers of Holocene vegetational change near the prairie–
966 forest ecotone in Minnesota: revisiting McAndrews' transect. *New Phytologist* 179, 449–459.
967 <https://doi.org/10.1111/j.1469-8137.2008.02482.x>

968 Nelson, D.M., Hu, F.S., Grimm, E.C., Curry, B.B., Slate, J.E., 2006. The Influence of Aridity and Fire on
969 Holocene Prairie Communities in the Eastern Prairie Peninsula. *Ecology* 87, 2523–2536.
970 [https://doi.org/10.1890/0012-9658\(2006\)87\[2523:TIOAAF\]2.0.CO;2](https://doi.org/10.1890/0012-9658(2006)87[2523:TIOAAF]2.0.CO;2)

971 NOAA (2023) NOW Data for Angola, IN. Available at: <https://www.weather.gov/wrh/climate?wfo=iwx>
972 (Accessed: 15 August 2023)

973 Nobel, P.S., 1983. *Biophysical Plant Physiology and Ecology*.

974 Nowacki, G.J., Abrams, M.D., 2008. The Demise of Fire and “Mesophication” of Forests in the Eastern
975 United States. *BioScience* 58, 123–138. <https://doi.org/10.1641/B580207>

976 Oswald, W.W., Doughty, E.D., Foster, D.R., Shuman, B.N., Wagner, D.L., 2017. Evaluating the role of
977 insects in the middle-Holocene *Tsuga* decline. *Journal of the Torrey Botanical Society*.

978 Oswald, W.W., Foster, D.R., 2012. Middle-Holocene dynamics of *Tsuga canadensis* (eastern hemlock) in
979 northern New England, USA. *The Holocene* 22, 71–78.
980 <https://doi.org/10.1177/0959683611409774>

981 Paciorek, C.J., Goring, S.J., Thurman, A.L., Cogbill, C.V., Williams, J.W., Mladenoff, D.J., Peters, J.A., Zhu,
982 J., McLachlan, J.S., 2016. Statistically-Estimated Tree Composition for the Northeastern United
983 States at Euro-American Settlement. *PLOS ONE* 11, e0150087.
984 <https://doi.org/10.1371/journal.pone.0150087>

985 Payette, S., 2021. A Paleo-perspective on Ecosystem Collapse in Boreal North America, in: Canadell, J.G.,
986 Jackson, R.B. (Eds.), *Ecosystem Collapse and Climate Change*, Ecological Studies. Springer
987 International Publishing, Cham, pp. 101–129. https://doi.org/10.1007/978-3-030-71330-0_5

988 Prentice, I.C., 1988. Records of vegetation in time and space: the principles of pollen analysis. *Vegetation
989 History, Handbook of Vegetation Science*.

990 Pribyl, P., Shuman, B.N., 2014. A computational approach to Quaternary lake-level reconstruction
991 applied in the central Rocky Mountains, Wyoming, USA. *Quaternary Research* 82, 249–259.
992 <https://doi.org/10.1016/j.yqres.2014.01.012>

993 Puleo, P.J.K., Axford, Y., McFarlin, J.M., Curry, B.B., Barklage, M., Osburn, M.R., 2020. Late glacial and
994 Holocene paleoenvironments in the midcontinent United States, inferred from Geneva Lake leaf
995 wax, ostracode valve, and bulk sediment chemistry. *Quaternary Science Reviews* 241, 106384.
996 <https://doi.org/10.1016/j.quascirev.2020.106384>

997 R Core Team (2021). R: A language and environment for statistical computing. R Foundation for
998 Statistical Computing, Vienna, Austria. URL <https://www.R-project.org/>.

999 Ramiadantsoa, T., Stegner, M.A., Williams, J.W., Ives, A.R., 2019. The potential role of intrinsic processes
1000 in generating abrupt and quasi-synchronous tree declines during the Holocene. *Ecology* 100,
1001 e02579. <https://doi.org/10.1002/ecy.2579>

1002 Ratajczak, Z., Carpenter, S.R., Ives, A.R., Kucharik, C.J., Ramiadantsoa, T., Stegner, M.A., Williams, J.W.,
1003 Zhang, J., Turner, M.G., 2018. Abrupt Change in Ecological Systems: Inference and Diagnosis.
1004 *Trends in Ecology & Evolution* 33, 513–526. <https://doi.org/10.1016/j.tree.2018.04.013>

1005 Ray-Cozzens 2022 - Ray-Cozzens, T., Stratigraphic evidence of water-level changes in small lakes in the
1006 Southern Great Lakes Region during the Late-Quaternary, Master's thesis, University of
1007 Wyoming Department of Geology and Geophysics, May 2022.

1008 Reimer, P.J., Austin, W.E.N., Bard, E., Bayliss, A., Blackwell, P.G., Ramsey, C.B., Butzin, M., Cheng, H.,
1009 Edwards, R.L., Friedrich, M., Grootes, P.M., Guilderson, T.P., Hajdas, I., Heaton, T.J., Hogg, A.G.,
1010 Hughen, K.A., Kromer, B., Manning, S.W., Muscheler, R., Palmer, J.G., Pearson, C., Plicht, J. van
1011 der, Reimer, R.W., Richards, D.A., Scott, E.M., Southon, J.R., Turney, C.S.M., Wacker, L., Adolphi,
1012 F., Büntgen, U., Capano, M., Fahrni, S.M., Fogtmann-Schulz, A., Friedrich, R., Köhler, P., Kudsk, S.,
1013 Miyake, F., Olsen, J., Reinig, F., Sakamoto, M., Sookdeo, A., Talamo, S., 2020. The IntCal20
1014 Northern Hemisphere Radiocarbon Age Calibration Curve (0–55 cal kBP). *Radiocarbon* 62, 725–
1015 757. <https://doi.org/10.1017/RDC.2020.41>

1016 Reimer, R.W. and Reimer, P.J. 2023 CALIBomb [WWW program] at <http://calib.org> accessed 2023-07-07

1017 Romme, W.H., Boyce, M.S., Gresswell, R., Merrill, E.H., Minshall, G.W., Whitlock, C., Turner, M.G., 2011.
1018 Twenty Years After the 1988 Yellowstone Fires: Lessons About Disturbance and Ecosystems.
1019 *Ecosystems* 14, 1196–1215. <https://doi.org/10.1007/s10021-011-9470-6>

1020 Schafstall, N., Kuosmanen, N., Fettig, C.J., Knižek, M., Clear, J.L., 2020. Late Glacial and Holocene records
1021 of tree-killing conifer bark beetles in Europe and North America: Implications for forest
1022 disturbance dynamics. *The Holocene* 0959683620902214.
1023 <https://doi.org/10.1177/0959683620902214>

1024 Seeley, M., Goring, S., Williams, J.W., 2019. Assessing the environmental and dispersal controls on *Fagus*
1025 *grandifolia* distributions in the Great Lakes region. *Journal of Biogeography* 46, 405–419.
1026 <https://doi.org/10.1111/jbi.13491>

1027 Shuman, B., 2012. Patterns, processes, and impacts of abrupt climate change in a warm world: the past
1028 11,700 years. *WIREs Climate Change* 3, 19–43. <https://doi.org/10.1002/wcc.152>

1029 Shuman, B. N., Stefanescu, I. C., Grigg, L. D., Foster, D. R., & Oswald, W. W. (2023). A millennial-scale
1030 oscillation in latitudinal temperature gradients along the western North Atlantic during the mid-
1031 Holocene. *Geophysical Research Letters*, 50, e2022GL102556.
1032 <https://doi.org/10.1029/2022GL102556>

1033 Shuman, B.N., Marsicek, J., Oswald, W.W., Foster, D.R., 2019. Predictable hydrological and ecological
1034 responses to Holocene North Atlantic variability. *Proceedings of the National Academy of
1035 Sciences* 116, 5985–5990. <https://doi.org/10.1073/pnas.1814307116>

1036 Shuman, B.N., Marsicek, J., 2016. The structure of Holocene climate change in mid-latitude North
1037 America. *Quaternary Science Reviews* 141, 38–51.
1038 <https://doi.org/10.1016/j.quascirev.2016.03.009>

1039 Shuman, B.N., Newby, P., Donnelly, J.P., 2009. Abrupt climate change as an important agent of
1040 ecological change in the Northeast U.S. throughout the past 15,000 years. *Quaternary Science
1041 Reviews* 28, 1693–1709. <https://doi.org/10.1016/j.quascirev.2009.04.005>

1042 Soil Survey (2023) Web Soil Survey, Natural Resources Conservation Service, United States Department
1043 of Agriculture. Available at: <https://websoilsurvey.nrcs.usda.gov/app/WebSoilSurvey.aspx>
1044 (Accessed: 31 March 2023)

1045 Sperry, J.S., Venturas, M.D., Anderegg, W.R.L., Mencuccini, M., Mackay, D.S., Wang, Y., Love, D.M., 2017.
1046 Predicting stomatal responses to the environment from the optimization of photosynthetic gain
1047 and hydraulic cost. *Plant, Cell & Environment* 40, 816–830. <https://doi.org/10.1111/pce.12852>

1048 Stafford, C.R., Richards, R.L., Anslinger, C.M., 2000. The Bluegrass Fauna and Changes in Middle
1049 Holocene Hunter-Gatherer Foraging in the Southern Midwest. *American Antiquity* 65, 317–336.
1050 <https://doi.org/10.2307/2694061>

1051 Stefanescu, I.C., Shuman, B.N., Grigg, L.D., Bailey, A., Stefanova, V., Oswald, W.W., 2023. Weak
1052 precipitation δ 2H response to large Holocene hydroclimate changes in eastern North America.
1053 *Quaternary Science Reviews* 304, 107990. <https://doi.org/10.1016/j.quascirev.2023.107990>

1054 Stephanson, C., Ribarik Coe, N., 2017. Impacts of Beech Bark Disease and Climate Change on American
1055 Beech. *Forests* 8, 155. <https://doi.org/10.3390/f8050155>

1056 Stuiver, M., 1968. Oxygen-18 Content of Atmospheric Precipitation during Last 11,000 Years in the Great
1057 Lakes Region. *Science* 162, 994–997. <https://doi.org/10.1126/science.162.3857.994>

1058 Surovell, T.A., Byrd Finley, J., Smith, G.M., Brantingham, P.J., Kelly, R., 2009. Correcting temporal
1059 frequency distributions for taphonomic bias. *Journal of Archaeological Science* 36, 1715–1724.
1060 <https://doi.org/10.1016/j.jas.2009.03.029>

1061 Transeau, E.N., 1935. The Prairie Peninsula. *Ecology* 16, 423–437. <https://doi.org/10.2307/1930078>

1062 Tubbs, C., Houston, D., 1990. *Fagus grandifolia* - American Beech, in: *Silvics of North America*. USDA.

1063 van Geel, B., Engels, S., Martin-Puertas, C., Brauer, A., 2013. Ascospores of the parasitic fungus

1064 *Kretzschmaria deusta* as rainstorm indicators during a late Holocene beech-forest phase around

1065 lake Meerfelder Maar, Germany. *J Paleolimnol* 50, 33–40. <https://doi.org/10.1007/s10933-013-9701-2>

1067 Valle, D., Baiser, B., Woodall, C.W., Chazdon, R., 2014. Decomposing biodiversity data using the Latent

1068 Dirichlet Allocation model, a probabilistic multivariate statistical method. *Ecology Letters* 17,

1069 1591–1601. <https://doi.org/10.1111/ele.12380>

1070 Vander Yacht, A.L., Keyser, P.D., Barrioz, S.A., Kwit, C., Stambaugh, M.C., Clatterbuck, W.K., Simon, D.M.,

1071 2019. Reversing Mesophication Effects on Understory Woody Vegetation in Mid-Southern Oak

1072 Forests. *Forest Science* 65, 289–303. <https://doi.org/10.1093/forsci/fxy053>

1073 Vose, J.M., Elliott, K.J., 2016. Oak, Fire, and Global Change in the Eastern USA: What Might the Future

1074 Hold? *fire ecol* 12, 160–179. <https://doi.org/10.4996/fireecology.1202160>

1075 Wang, Y., Gill, J.L., Marsicek, J., Dierking, A., Shuman, B., Williams, J.W., 2016. Pronounced variations in

1076 *Fagus grandifolia* abundances in the Great Lakes region during the Holocene. *The Holocene* 26,

1077 578–591. <https://doi.org/10.1177/0959683615612586>

1078 Webb, T., Cushing, E.J., Wright, H.E., 1984. Holocene Changes in the Vegetation of the Midwest, in:

1079 Wright, H.E. (Ed.), *Late Quaternary Environments of the United States, Volume 2*. University of

1080 Minnesota Press, pp. 142–165.

1081 Weiwei, L.U., Xinxiao, Y.U., Guodong, J.I.A., Hanzhi, L.I., Ziqiang, L.I.U., 2018. Responses of Intrinsic

1082 Water-use Efficiency and Tree Growth to Climate Change in Semi-Arid Areas of North China. *Sci*

1083 *Rep* 8, 308. <https://doi.org/10.1038/s41598-017-18694-z>

1084 Westerling, A.L., Turner, M.G., Smithwick, E.A.H., Romme, W.H., Ryan, M.G., 2011. Continued warming

1085 could transform Greater Yellowstone fire regimes by mid-21st century. *Proceedings of the*

1086 *National Academy of Sciences* 108, 13165–13170. <https://doi.org/10.1073/pnas.1110199108>

1087 Whitlock, C., Larsen, C., 2001. Charcoal as a Fire Proxy, in: *Tracking Environmental Change Using Lake*

1088 *Sediments. Vol. 3: Terrestrial, Algal, and Siliceous Indicators.* pp. 75–97.

1089 https://doi.org/10.1007/0-306-47668-1_5

1090 Widhalm, M., Hamlet, A. Byun, K., Robeson, S., Baldwin, M., Staten, P., Chiu, C., Coleman, J., Hall, E.,

1091 Hoogewind, K., Huber, M., Kieu, C., Yoo, J., Dukes, J.S., 2018. Indiana's Past & Future Climate: A

1092 Report from the Indiana Climate Change Impacts Assessment. Purdue Climate Change Research
1093 Center, Purdue University. West Lafayette, Indiana. DOI: 10.5703/1288284316634

1094 Wiles, S. (2023) History in the Margins: Ecotonal Dynamics and Abrupt Vegetation Change in Holocene
1095 Lower Michigan, M.S. Thesis, University of Wisconsin – Madison, Department of Geography.

1096 Williams, A.S., 1974. Late-glacial Postglacial Vegetational History of the Pretty Lake Region, Northeastern
1097 Indiana (Geological Survey Professional Paper), Professional Paper.

1098 Williams, J.W., B. Shuman, P. Bartlein, J. Whitmore, K. Gajewski, M. Sawada, T. Minckley, S. Shafer, A.
1099 Viau, T. Webb, P. Anderson, L. Brubaker, C. Whitlock, & O. Davis. (2006). An Atlas of Pollen–
1100 Vegetation–Climate Relationships for the United States and Canada.

1101 Williams, J.W., Blois, J.L., Shuman, B.N., 2011. Extrinsic and intrinsic forcing of abrupt ecological change:
1102 case studies from the late Quaternary. *Journal of Ecology* 99, 664–677.
1103 <https://doi.org/10.1111/j.1365-2745.2011.01810.x>

1104 Williams, J.W., Jackson, S.T., 2007. Novel climates, no-analog communities, and ecological surprises.
1105 *Frontiers in Ecology and the Environment* 5, 475–482. <https://doi.org/10.1890/070037>

1106 Williams, J.W., Shuman, B., Bartlein, P.J., 2009. Rapid responses of the prairie-forest ecotone to early
1107 Holocene aridity in mid-continental North America. *Global and Planetary Change* 66, 195–207.
1108 <https://doi.org/10.1016/j.gloplacha.2008.10.012>

1109 Williams, J.W., Shuman, B., Bartlein, P.J., Diffenbaugh, N.S., Webb, T., III, 2010. Rapid, time-
1110 transgressive, and variable responses to early Holocene midcontinental drying in North America.
1111 *Geology* 38, 135–138. <https://doi.org/10.1130/G30413.1>

1112

1113 **Tables**

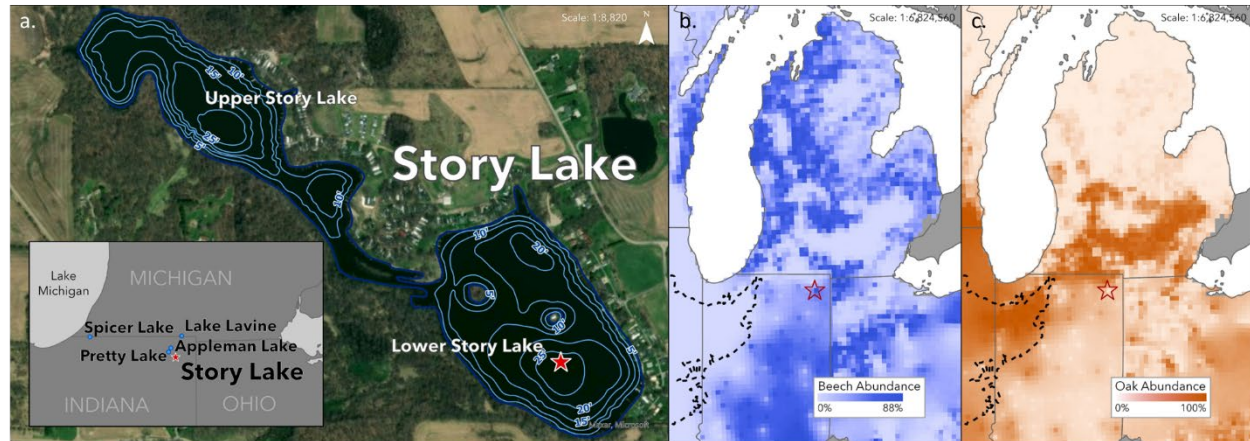
1114 Table 1: List of all macrofossils and radiocarbon dates and additional points used to build the age–depth
 1115 model for Story Lake, Indiana. The date that was identified by the age-depth model as an outlier is
 1116 indicated with an asterisk (*), radiocarbon dates that represent post-1950 CE samples (identified with a
 1117 cross †) have age estimates were provided by *CALIBomb*. NA indicates that there is no radiocarbon date
 1118 associated with that sample either because the sample does not come from radiocarbon dated material
 1119 (coretop and *Ambrosia* rise), the two samples determined to be modern (27.5 cm and 29.5 cm), and a
 1120 sample that was too small for dating (642.5 cm). Calibrated years BP is equal to the mean $\pm 1\sigma$ or for ^{14}C
 1121 the calibrated median age (years before 1950 CE)

1122

Laboratory ID	Core Depth (cm of sample midpoint)	^{14}C age and error (radiocarbon years before 1950 CE)	Calibrated years BP	95% Calibrated credible interval age range (year BP)	Dated material
Coretop	0.5	NA	-69 \pm 10	NA	Core top
STOR191A1B-27.5	27.5	NA	-21 \pm 12†	NA	Leaf fragment
STOR191A1B-29.5	29.5	NA	-21 \pm 12†	NA	Leaf fragment
STOR191A2L-128.5	128.5	NA	90 \pm 25	NA	<i>Ambrosia</i> rise
STOR191A2L-138.5	138.5	170 \pm 15	187	5-279	Leaf fragment
STOR191A2L-151.5	151.5	400 \pm 60	440	315-523	Wood fragment
STOR191A2L-181.5	181.5	970 \pm 15	851	801-920	Root fragment
STOR191A3L-262.5	262.5	2085 \pm 15	2040	1996-2108	Fibrous plant
STOR191A2L-296.5	296.5	2505 \pm 15	2576	2501-2716	Fibrous plant
STOR191A2L-304.5	304.5	2530 \pm 20	2620	2509-2729	Fibrous plant
STOR191A4L-332.5	332.5	42440 \pm 840*	45093	43591-46554	Fibrous plant
STOR191A6L-519.5	519.5	4590 \pm 60	5296	5052-5461	Leaf fragment
STOR191C6L-575.5	575.5	5520 \pm 25	6308	6283-6389	Leaf fragment
STOR191A2L-615.5	615.5	6270 \pm 70	7183	6992-7333	Leaf fragment
STOR191A2L-642.5	642.5	NA	NA	NA	Plant fiber

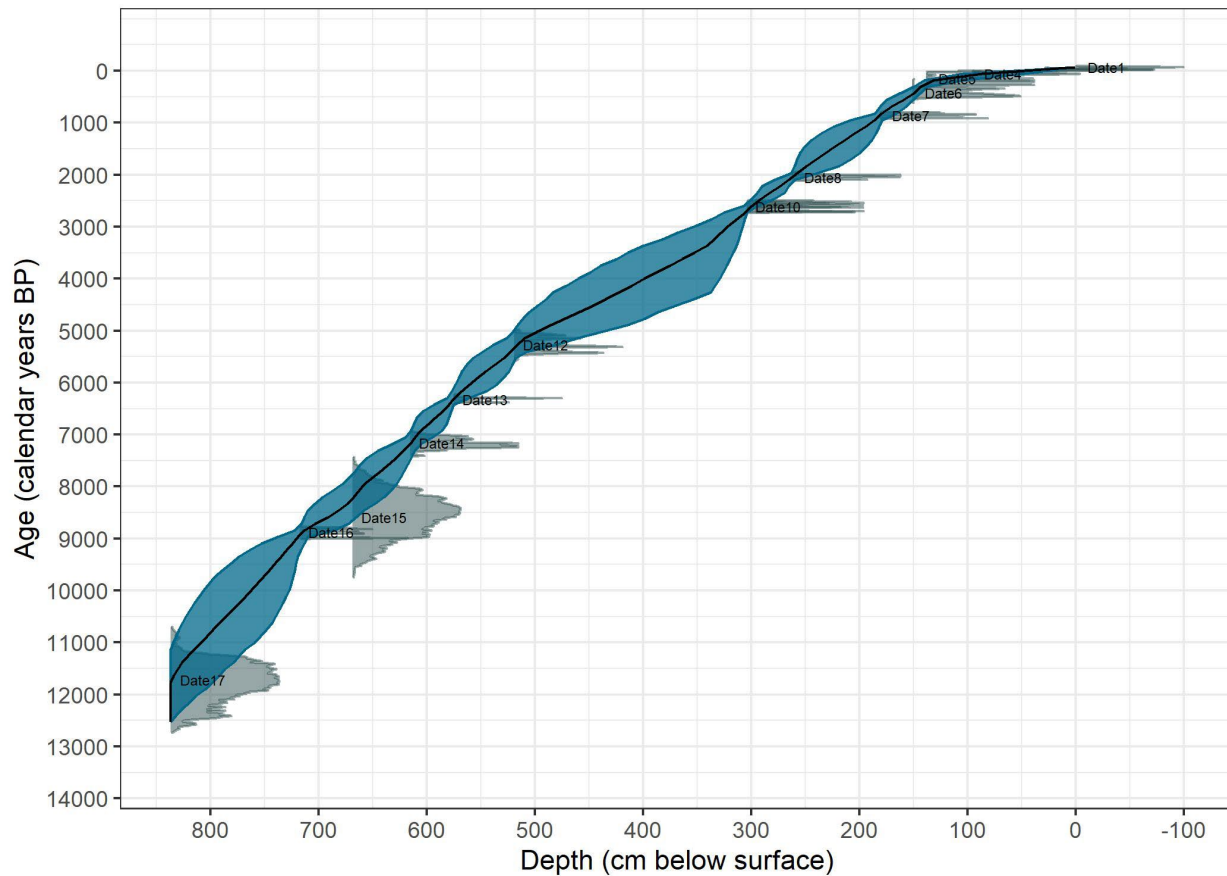
STOR191A8L-668.5	668.5	7660 ± 360	8524	7808-9373	Leaf fragment
STOR191A8L-717.5	717.5	8025 ± 20	8890	8781-9001	Wood fragment
STOR191A9L-836.5	836.5	10110 ± 210	11740	11124-12519	Cone fragment

1123 **Figures**



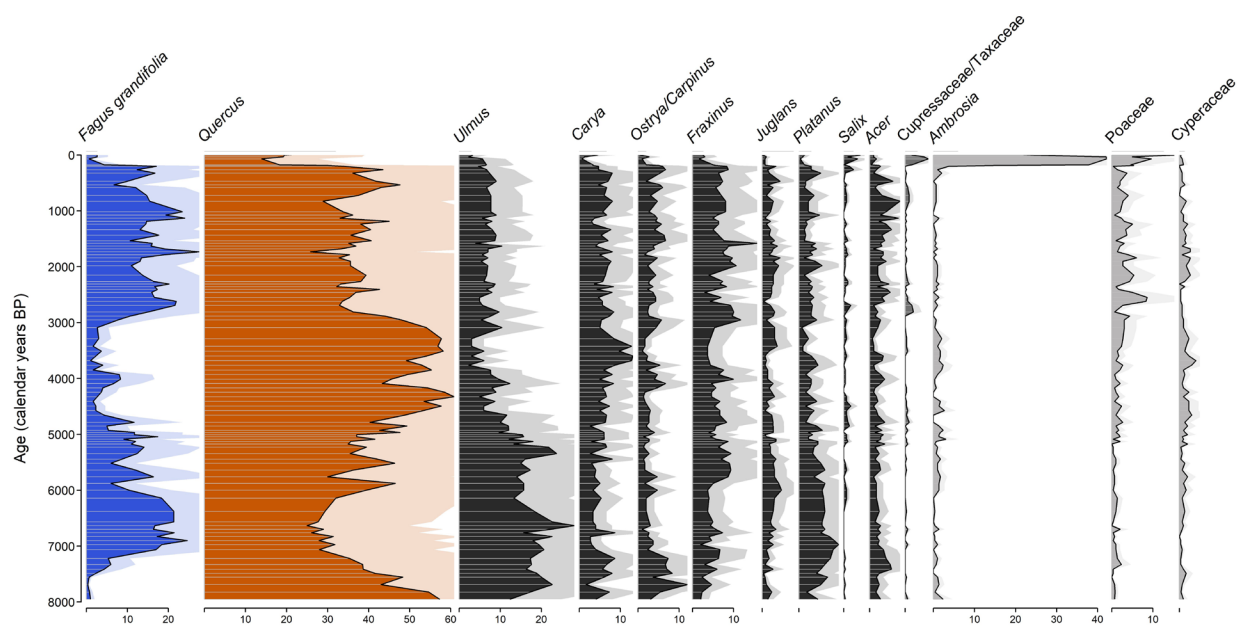
1124

1125 Figure 1: Panel a shows the coring location for Story Lake, Indiana (IN), with bathymetric contours showing
 1126 lake depths in 1.52m (5 foot) increments (blue lines, IDNR 2019). Inset map shows location of Story Lake
 1127 (red star) and four comparison sites: Lake Lavine, MI, Spicer Lake, IN, Appleman Lake, IN, and Pretty Lake,
 1128 IN (blue points). Panels b and c show the location of Story Lake relative to pre-settlement distributions of
 1129 American beech (middle) and oak (right; Paciorek et al. 2016). The dashed line indicates the boundary of
 1130 the temperate prairie parkland from the USDA Ecological Subregions (McNab et al. 2007). Areal imagery
 1131 Sources: Esri, DigitalGlobe, GeoEye, i-cubed, USDA FSA, USGS, AEX, Getmapping, Aerogrid, IGN, IGP,
 1132 swisstopo, and the GIS User Community.

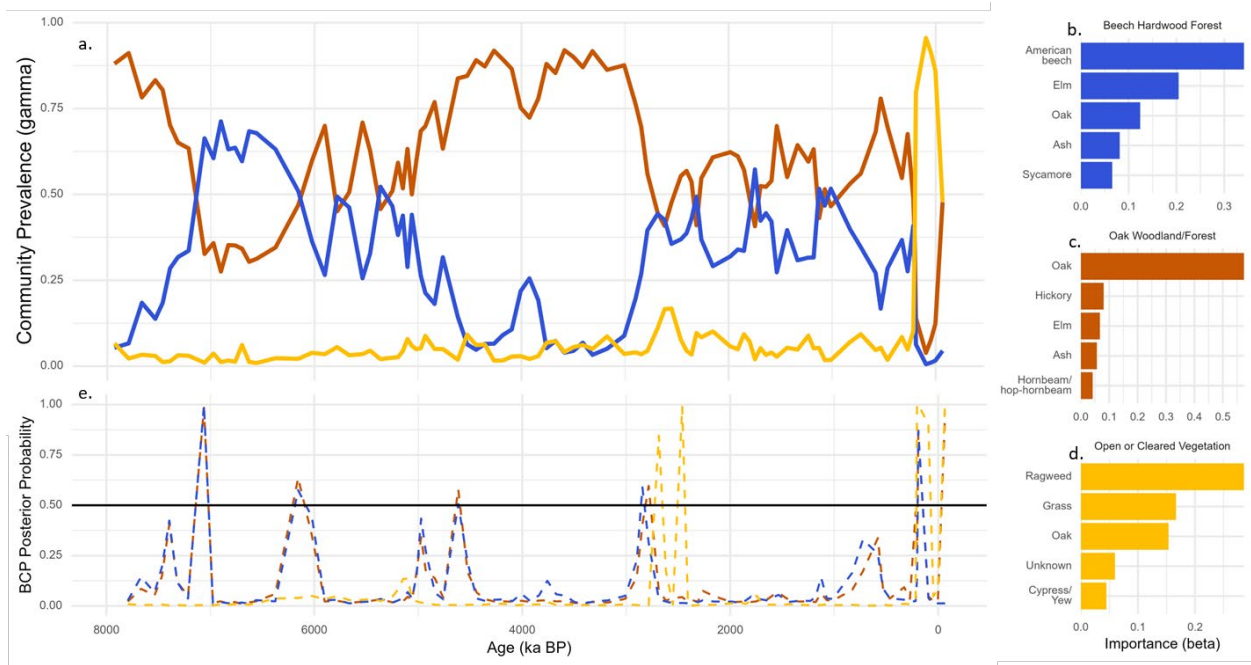


1133

1134 Figure 2: Age-depth model for Story Lake, based on the *bchron* R package (Haslett and Parnell, 2008),
 1135 constructed from 17 age controls (15 ^{14}C dates, *Ambrosia* rise, coretop, Table 1), shows a continuous
 1136 sediment record spanning from 11.7 ka BP to present with an average deposition time of 9.25 years/cm.
 1137 Individual radiocarbon dates are shown as the density distributions of their calibrated ages (grey). The
 1138 95% confidence interval of the age-depth model is shown in blue. One ^{14}C date at 332.5 cm was
 1139 determined as an outlier by *bchron* (Table 1) and is not shown here.



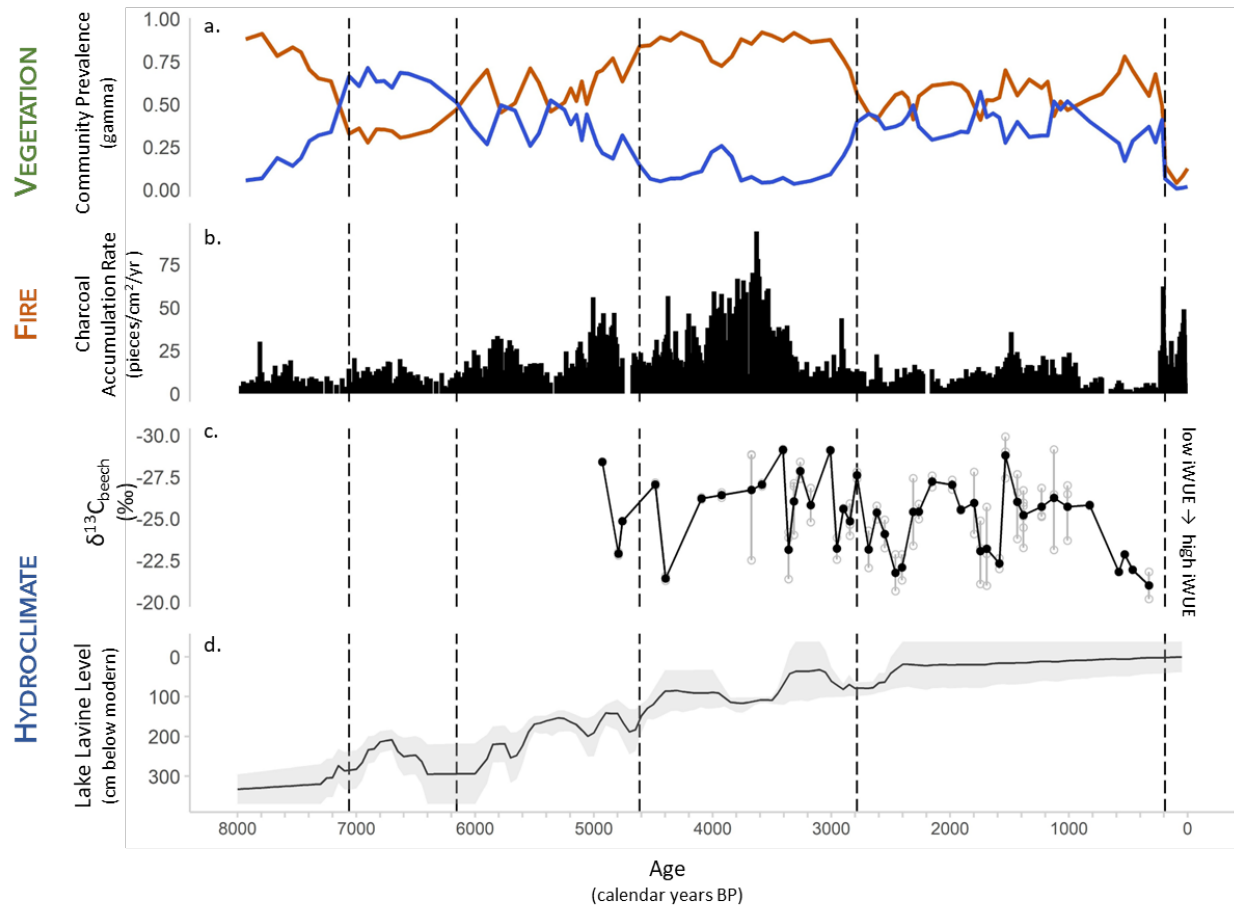
1140
1141 Figure 3: Pollen percentages of major taxa (>3.5% abundance) for Story Lake, Indiana from 8 to 0 ka BP.
1142 American beech (*Fagus grandifolia*, blue) and oak (*Quercus*, orange) are highlighted. Arboreal pollen types
1143 have a black fill, while non-arboreal pollen types have a gray fill. Exaggerated pollen percent
1144 x2 are shown in lighter colors. Individual samples are indicated by horizontal light lines.

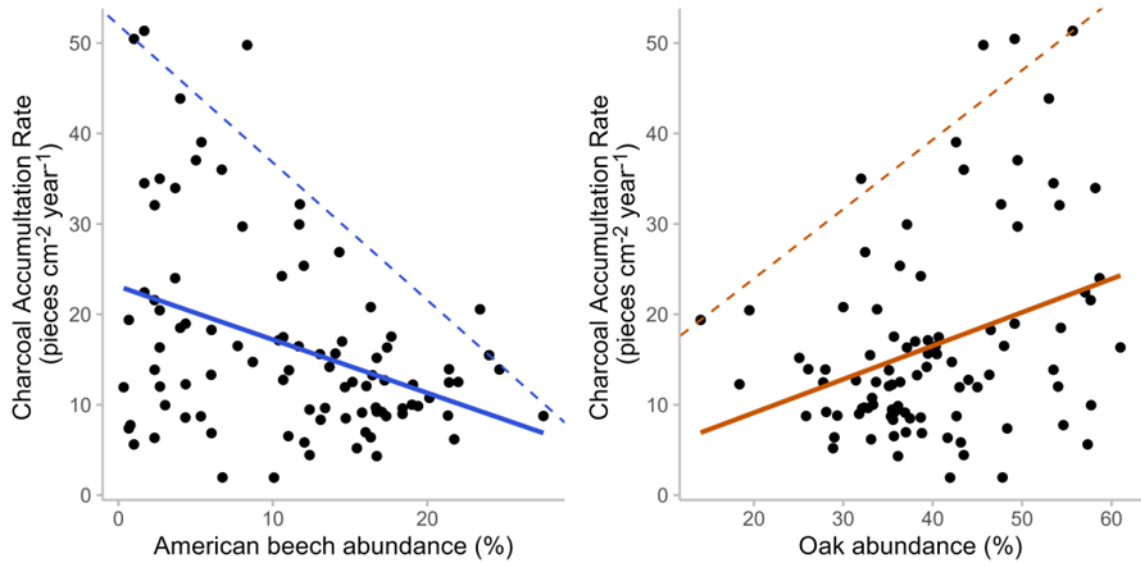


1145

1146 Figure 4: Prevalence of vegetation types through time at Story Lake as identified by the CTM topic model
 1147 (panel a). Colors correspond to vegetation types: beech-hardwood forest (blue), oak forest/woodland
 1148 (orange), and open/cleared vegetation (yellow). The importance of taxa within each vegetation type is
 1149 displayed as bar graphs (panels b-d). Dashed lines in panel e show the probability of change points for
 1150 each community type based on Bayesian change point analysis, with the black horizontal bar indicating
 1151 the 0.5 posterior probability threshold used to identify change points.

1152

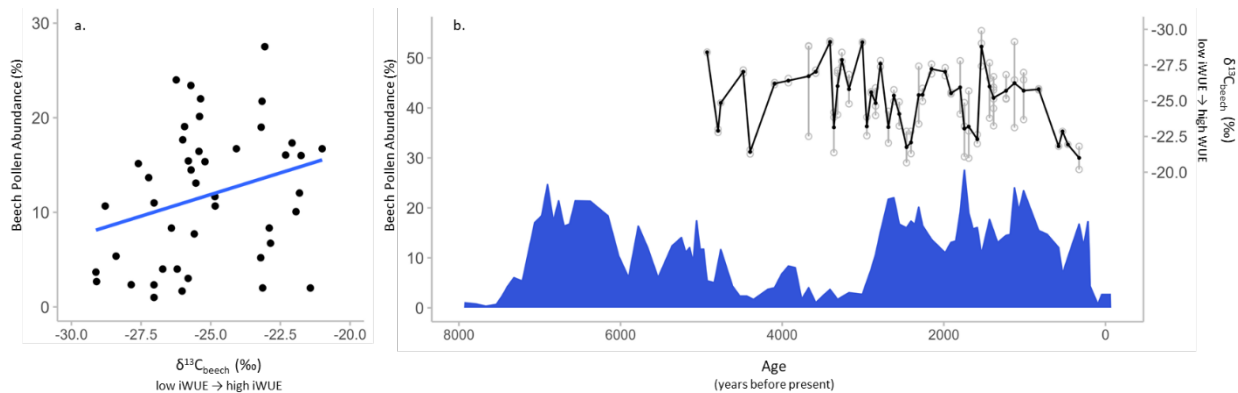




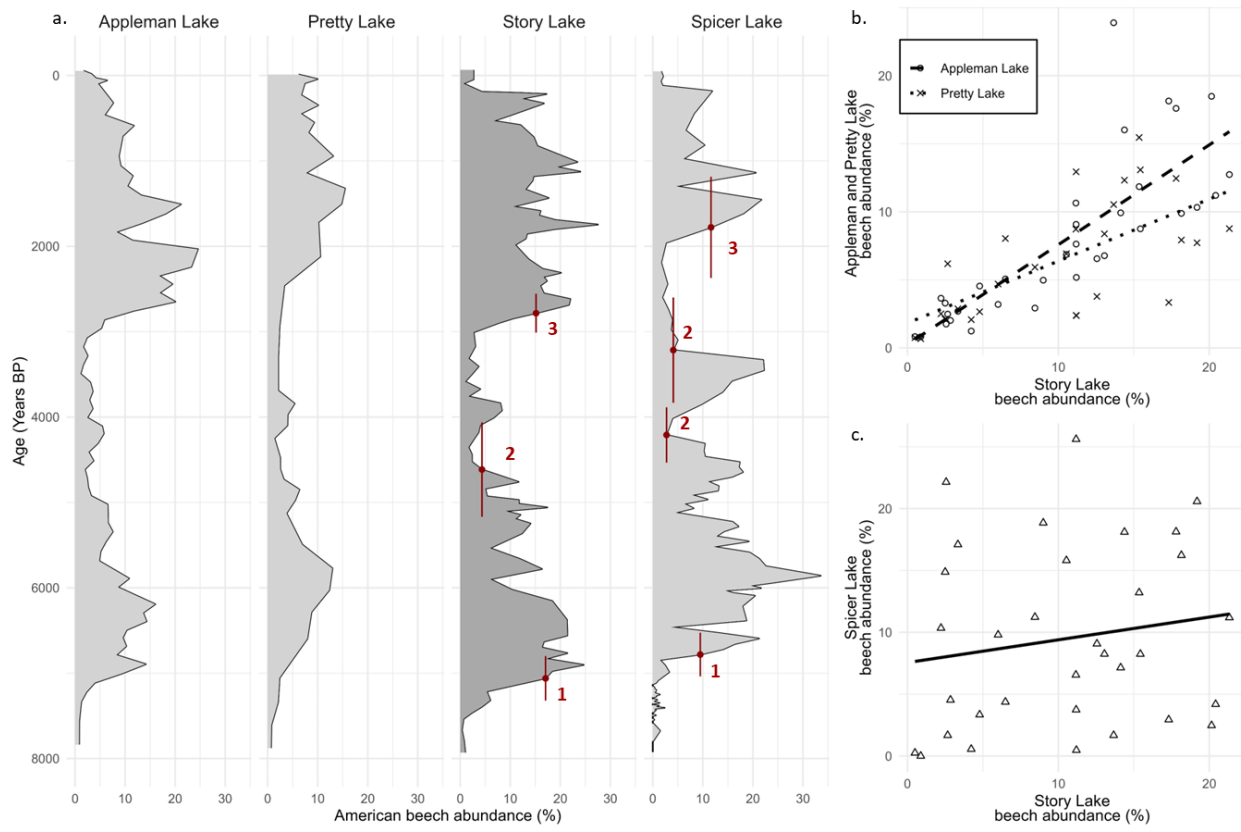
1163

1164 Figure 6: Correlation between charcoal accumulation rate and American beech (*Fagus grandifolia*)
 1165 abundance (left, p-value < 0.001, $r^2 = 0.14$, Pearson's correlation = -0.38) and oak (*Quercus*) abundance
 1166 (right, p-value < 0.001, $r^2 = 0.11$, Pearson's correlation = 0.33). Dashed lines represent the 95th quantile
 1167 regression.

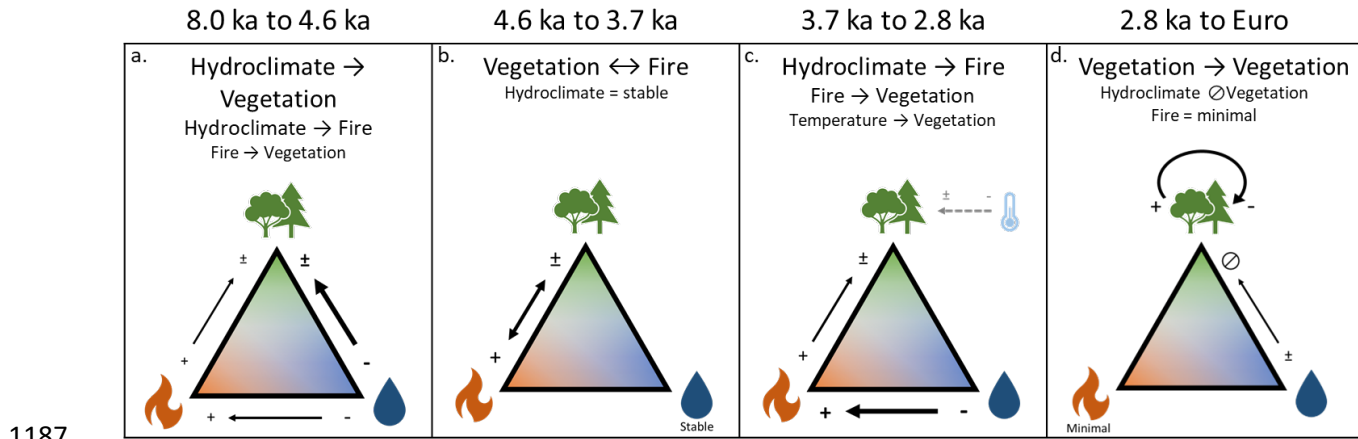
1168



1171 Figure 7: Comparison of American beech (*Fagus grandifolia*) pollen abundance (panel a, y-axis and panel
 1172 b left y-axis) and $\delta^{13}\text{C}$ of American beech pollen grains ($\delta^{13}\text{C}_{\text{beech}}$, panel a x-axis and panel b right y-axis).
 1173 Individual aliquots of $\delta^{13}\text{C}_{\text{beech}}$ are shown on panel b, indicated by grey hollow circles connected by a
 1174 vertical line. Direct comparison of American beech abundance and $\delta^{13}\text{C}_{\text{beech}}$ (panel a) shows no significant
 1175 correlation (p-value = 0.06, $r^2 = 0.06$, Pearson's correlation = 0.28).



1178 Figure 8: a) Comparison of Holocene variations in American beech (*Fagus grandifolia*) pollen abundances
 1179 for Story Lake and nearby Appleman and Pretty Lakes, and the more distal lake, Spicer Lake. To compare
 1180 regional timing of beech fluctuations, red bars represent the 95% confidence interval as inferred by *bchron*
 1181 for selected points in the Story and Spicer Lake records with possible visual correspondences: the initial
 1182 early-Holocene rise (1), the beginning of the mid-Holocene low period compared to two potential matches
 1183 in the Spicer Lake record (2) and the end of the mid-Holocene low (3). b) Correlation of American beech
 1184 abundance between Story Lake and local lakes, Appleman ($p\text{-value} < 0.05$, $r^2 = 0.64$, Pearson's correlation
 1185 = 0.80) and Pretty ($p\text{-value} < 0.05$, $r^2 = 0.44$, Pearson's correlation = 0.66). c) Correlation of American beech
 1186 abundance between Story Lake and Spicer Lake ($p\text{-value} = 0.39$, $r^2 = 0.03$, Pearson's correlation = 0.15).



1188 Figure 9: Schematic diagram, showing interpretation of the changing drivers and vegetation-fire-
 1189 hydroclimate feedbacks of ecological change at different time periods (a-d) at Story Lake, Indiana.
 1190 Regional-scale temperature changes, which were not directly analyzed here, but which may modulate
 1191 these feedbacks are identified by a grey dashed arrow. The hypothesized relative importance of each
 1192 factor is depicted by arrow width and font size.